Protein phosphatase 6 regulates mitotic spindle formation by controlling the T-loop phosphorylation state of Aurora A bound to its activator TPX2

Kang Zeng, Ricardo Nunes Bastos, Francis A. Barr, and Ulrike Gruneberg

University of Liverpool, Cancer Research Centre, Liverpool L3 9TA, England, UK

Many protein kinases are activated by a conserved regulatory step involving T-loop phosphorylation. Although there is considerable focus on kinase activator proteins, the importance of specific T-loop phosphatases reversing kinase activation has been underappreciated. We find that the protein phosphatase 6 (PP6) holoenzyme is the major T-loop phosphatase for Aurora A, an essential mitotic kinase. Loss of PP6 function by depletion of catalytic or regulatory subunits interferes with spindle formation and chromosome alignment because of increased Aurora A activity. Aurora A T-loop phosphorylation and the stability of the Aurora A–TPX2 complex are increased in cells depleted of PP6 but not other phosphatases. Furthermore, purified PP6 acts as a T-loop phosphatase for Aurora A–TPX2 complexes in vitro, whereas catalytically inactive mutants cannot dephosphorylate Aurora A or rescue the PPP6C depletion phenotype. These results demonstrate a hitherto unappreciated role for PP6 as the T-loop phosphatase regulating Aurora A activity during spindle formation and suggest the general importance of this form of regulation.

Introduction

Dynamic protein phosphorylation, mediated by a conserved cohort of protein kinases, controls the profound changes in cellular organization required for mitosis and cytokinesis (Nigg, 2001). Many of these kinases share a common activation mechanism involving phosphorylation of a threonine residue within the activation or T loop and binding to a coactivator protein (Fig. 1 A; Gold et al., 2006). These events promote the positioning of key residues required for the phosphotransfer reaction from ATP bound in the kinase active site to the acceptor residue in the substrate protein (Huse and Kuriyan, 2002). T-loop phosphorylation can be autocatalytic or mediated by an upstream kinase and generally increases kinase activity by several orders of magnitude (Adams, 2003). Recent studies on the activation of Aurora A exemplify the importance of T-loop phosphorylation as a regulatory mechanism (Bayliss et al., 2003; Eyers et al., 2003). Aurora A is localized to the centrosomes and spindle poles from late S phase throughout mitosis, which is consistent with its function in organizing mitotic spindle formation (Glover et al., 1995; Giet et al., 2002). Localization to the spindle is achieved through the association of Aurora A with its binding partner TPX2 (Kufer et al., 2002). Besides this targeting function, TPX2 is critically important for autocatalytic phosphorylation of threonine 288 in the T loop of Aurora A and, hence, Aurora A activation (Bayliss et al., 2003; Eyers et al., 2003). Furthermore, TPX2 also prevents the dephosphorylation of this residue (Bayliss et al., 2003; Eyers et al., 2003). Other interaction partners of Aurora A, such as PAK1, Ajuba, and Bora, have also been reported to facilitate T288 phosphorylation, although the structural basis for these effects is not yet known (Hirota et al., 2003; Zhao et al., 2005; Hutterer et al., 2006). Consistent with the function of Aurora A in spindle pole maturation and separation, T288-phosphorylated and, hence, activated Aurora A can be detected at the spindle poles (Ohashi et al., 2006). Several potential Aurora A substrates on mitotic spindles have been described previously, including the BimC family kinesin KIF11/Eg5 (Giet et al., 1999, 2002; Kinoshita et al., 2005). Because KIF11/Eg5 is critically required for spindle

F.A. Barr and U. Gruneberg contributed equally to this paper.

Correspondence to Francis A. Barr: fabarr@liv.ac.uk; or Ulrike Gruneberg: u.gruneberg@liv.ac.uk

Abbreviations used in this paper: PPP, phosphoprotein phosphatase; SAPS, SIT4 phosphatase–associated protein.

© 2010 Zeng et al. This article is distributed under the terms of an Attribution–Noncommercial–Share Alike–No Mirror Sites license for the first six months after the publication date (see http://www.rupress.org/terms). After six months it is available under a Creative Commons License (Attribution–Noncommercial–Share Alike 3.0 Unported license, as described at http://creativecommons.org/licenses/by-nc-sa/3.0/).

The Rockefeller University Press $30.00
J. Cell Biol. Vol. 191 No. 7 1315–1332
www.jcb.org/cgi/doi/10.1083/jcb.201008106

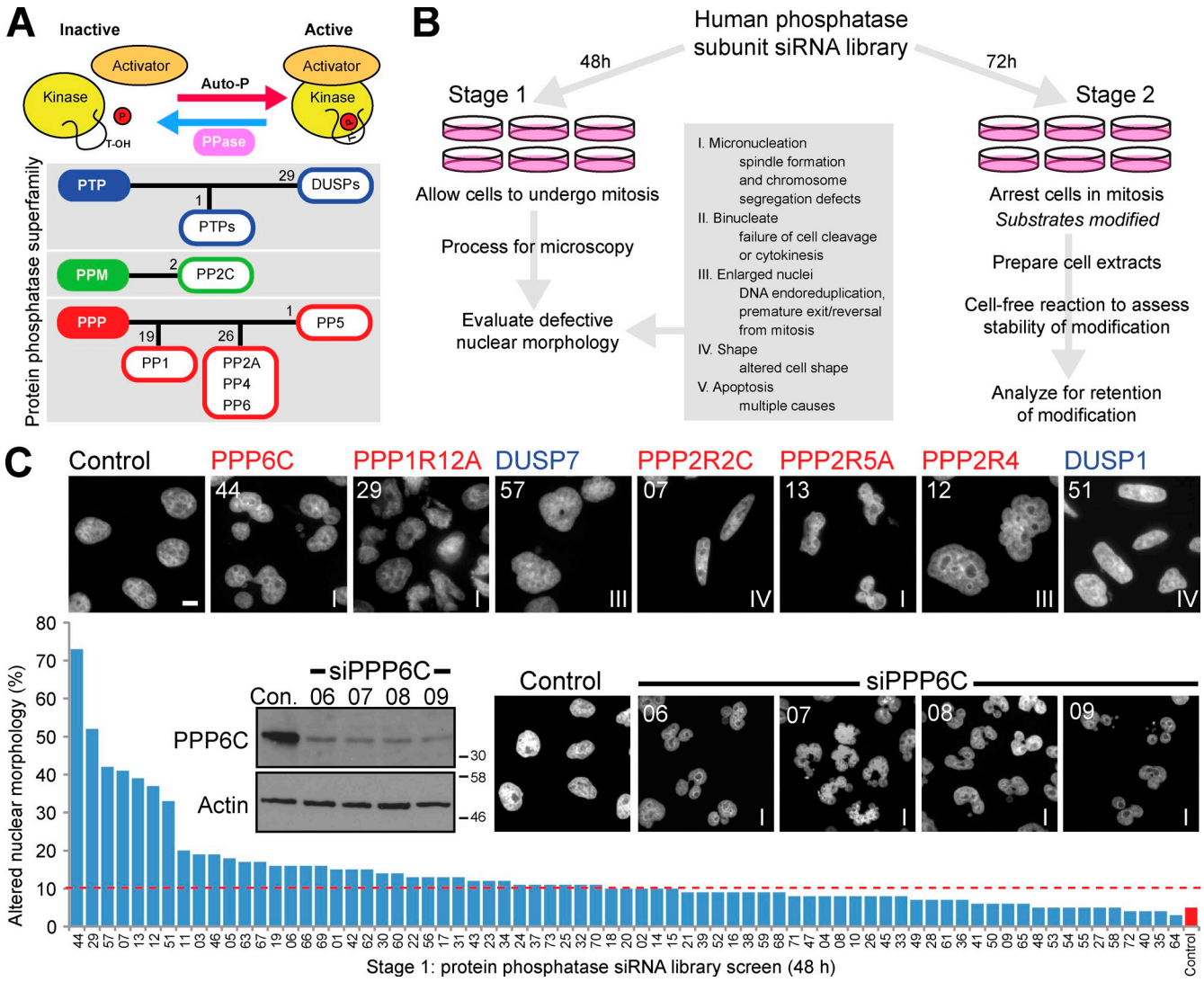

Figure 1. **Identification of human phosphatases required for normal mitosis.** (A) A model for the T loop–mediated kinase activation. Below is a schematic of the human protein phosphatase superfamily covering the phosphoprotein phosphatases (PPP), the metallophosphatases (PPM), and the phosphotyrosine protein (PTP) and dual-specificity phosphatases (DUSPs) modified from Chen et al. (2007). The number of phosphatase subunits screened in each subfamily is indicated. (B) The screening procedure and the phenotypes expected are categorized using Roman numerals together with a brief description of the underlying causes. (C) HeLa cells were transfected with siRNA pools for 78 human phosphatase subunits, fixed after 48 h, and stained with DAPI to reveal the DNA and nuclear morphology. Abnormal nuclear morphology was scored according to the categories (I–V) described and is expressed as a histogram sorted from high to low (n = 3). The dotted line indicates twice the median value for nuclear abnormalities. For verification, HeLa cells were transfected with the four siRNA duplexes (06–09) making up the PPP6C siRNA pool, fixed after 48 h, and then stained with DAPI to reveal the DNA and nuclear morphology. Numbers in the top left corner correspond to the siRNA library pool used. Con., control. Bar, 10 µm.

pole separation and bipolar spindle formation, a potential upstream regulatory role for Aurora A coordinating KIF11/Eg5 activity with that of other spindle assembly factors is an attractive model (Clarke and Zhang, 2008; Eckerdt et al., 2008).

Despite the recent advances in understanding how T-loop phosphorylation of the major mitotic kinases is accomplished (Gold et al., 2006), the opposing phosphatases remain largely elusive. The prevailing view is that dephosphorylation during mitosis is performed by phosphatase complexes of the phosphoprotein phosphatase (PPP) family (Bollen et al., 2009), making them good candidates for T-loop phosphatases. These enzymes consist of a catalytic subunit in complex with one or more regulatory subunits (Shi, 2009). The regulatory subunits confer localization and substrate specificity to these holoenzyme complexes, both increasing activity toward true substrates and reducing activity toward other phosphorylated proteins (Johnson et al., 1996; Hirano et al., 1997; Tóth et al., 2000; Terrak et al., 2004). To achieve a clearer understanding of the regulation of mitosis, it is therefore necessary to identify the specific phosphatase holoenzyme complexes opposing the key mitotic kinases. The recent identification of specific protein phosphatase 1 (PP1) and PP2A complexes regulating chromosome condensation and sister chromatid cohesion, respectively, has highlighted the importance of local dephosphorylation of kinase substrates during mitosis (Kitajima et al., 2006; Tang et al., 2006; Vagnarelli et al., 2006). In this study, we focus on the kinases themselves. Using an unbiased two-stage screen of protein phosphatase subunits, we search for T-loop phosphatase activities important for normal mitosis.

Results

Identification of phosphatases required for normal mitosis

Loss of T-loop phosphatase function for the essential mitotic kinases should cause defective spindle formation, chromosome alignment, and cytokinesis and, therefore, give rise to cells with characteristic nuclear abnormalities (Fig. 1 B, stage 1). To identify nonredundant protein phosphatases required for normal mitosis, a visual screen for cells with abnormal nuclei after 48-h siRNA-mediated depletion of phosphatase subunits was performed (Fig. 1, A–C). For this purpose, siRNA pools were used containing four different duplexes against the same target gene (Table S1). Of the phosphatase subunits tested, only seven gave rise to nuclear morphology defects with a frequency above a threshold set at twice the median value (Fig. 1 C). The most striking of these was the PP6 catalytic subunit (PPP6C), in which >70% of cells showed abnormally shaped fragmented nuclei but otherwise normal cell morphology (Fig. 1 C). Interestingly, a previous screen of phosphatases required for mitosis in *Drosophila melanogaster* found that PP6 depletion caused a twofold increase in the mitotic index, but its function was not investigated further in this study (Chen et al., 2007). Mutations in PP6 were recently also found to cause spindle position and cell contractility defects in *Caenorhabditis elegans* early embryonic cell divisions (Afshar et al., 2010). However, no substrates were identified. Of the other phosphatase subunits identified, PPP1R12A (MYPT1) has been reported to function as part of a PP1 holoenzyme complex in mitosis by opposing Plk1 (Yamashiro et al., 2008). Because the initial 48-h screen failed to pick the PP1 catalytic subunits, these were examined in more detail. At 72 h, the PPP1C-B catalytic subunit gave a nuclear morphology defect similar to PPP1R12A (Fig. S1 A), which was consistent with previous findings that MYPT1 binds to PPP1C-B (Hartshorne et al., 2004; Yamashiro et al., 2008). Although no obvious change was observed with PPP1C-A, PPP1C-C depletion resulted in alterations to the microtubule cytoskeleton and cell shape change without causing nuclear abnormalities (Fig. S1 A), suggesting that PP1 catalytic subunits have distinct functions.

The PP2A regulatory subunit PPP2R5A was also found in the screen. PP2A regulatory (PPP2R5/B56/B′ isoform) and catalytic subunits are present in the shugoshin complexes controlling centromeric cohesion (Kitajima et al., 2006). In this case, redundancy between the different PP2 catalytic subunits was observed (Fig. S1 B), explaining why they were not found in the initial screen. Depletion of both the A and B catalytic subunits of PP2A was necessary to cause cells to arrest in mitosis with scattered chromosomes (Fig. S1 B). Because the functions of PPP1R12A and PPP2R5A as part of PP1 and PP2A complexes, respectively, are already known (Kitajima et al., 2006; Yamashiro et al., 2008), it was therefore decided to focus on the category I phenotype seen with PPP6C.

To test whether the defect observed for PPP6C was both specific and indicative of a general function for this phosphatase in mitosis, additional verification steps were performed. When tested in isolation, all four of the single siRNA duplexes used in the pool were able to deplete PPP6C and cause the same altered nuclear morphology (Fig. 1 C, Western blot and bottom images). PP6 may therefore be a cell cycle regulator and a candidate T-loop phosphatase in human cells, and it was investigated further.

Analysis of the PP6 holoenzyme in mitosis

Like other PPP family members, PP6 is a multisubunit enzyme, comprising a single catalytic subunit and one of each of the three SIT4 phosphatase–associated protein (SAPS) domain regulatory subunits and three ankyrin repeat domain subunits (Stefansson and Brautigan, 2006; Stefansson et al., 2008). PP6 also interacts with α4, which has a chaperone-like activity required to maintain active PP2A, PP4, and PP6 (Prickett and Brautigan, 2006; Kong et al., 2009). To define which of these subunits are important for mitosis, PP6 holoenzyme complexes were isolated from mitotic cells stably expressing FLAG-tagged PPP6C and then analyzed by SDS-PAGE and mass spectrometry. This revealed that HeLa cells express all known PP6 subunits and that these are present in PPP6C complexes during mitosis (Fig. 2 A). To test whether the PP6 SAPS domain regulatory subunits and ankyrin repeat domain subunits are required for normal mitosis, they were depleted using siRNA. Western blotting revealed that these subunits could be depleted singly or in combination, but this did not alter the amount of the PP6 catalytic subunit present (Fig. 2 B). When all three SAPS domain regulatory subunits were depleted together, altered nuclear morphology similar to that seen after PPP6C depletion was observed (Fig. 2 C). Single depletions showed partially altered nuclear morphology (Fig. 2 C), supporting the idea that there is redundancy between these subunits. Depletion of the ANKRD52 subunit had no effect on nuclear morphology, whereas ANKRD28 and ANKRD44 ankyrin repeat subunit depletion altered nuclear morphology (Fig. 2 C). Collectively, these findings suggest that a PP6 holoenzyme, comprising PPP6C catalytic, SAPS1–3 regulatory, and ANKRD28–44 subunits, is required for normal mitotic progression.

PP6 activity is required for normal mitosis

The function of PP6 in mitosis could be explained by either a structural role or as an active phosphatase. To discriminate between these two possibilities, stable cell lines expressing either wild type (si08^{Res}PPP6C^{WT}) or catalytically inactive (si08^{Res}PPP6C^{PD}) mutant forms of the PP6 catalytic subunit were generated (Fig. 3 A). To enable depletion of the endogenous PP6 catalytic subunit, these constructs were engineered to be resistant to the PPP6C si08 duplex while retaining sensitivity to si07, to allow depletion of all PPP6C. When si08^{Res}PPP6C^{WT} cells were depleted of endogenous PPP6C using si08, the wild-type transgene was able to rescue the phenotype, and cells retained normal-shaped nuclei (Fig. 3 B). Depletion of all PPP6C using si07 gave the expected altered nuclear morphology. In contrast, when si08^{Res}PPP6C^{PD} cells were depleted of endogenous PPP6C using si08, the phosphatase-dead mutant transgene was unable to rescue the phenotype, and cells displayed abnormally shaped nuclei similar to wild-type HeLa cells treated with the same duplex (Fig. 3 B). Depletion of endogenous PPP6C by si07 and si08 and of the transgene-expressed

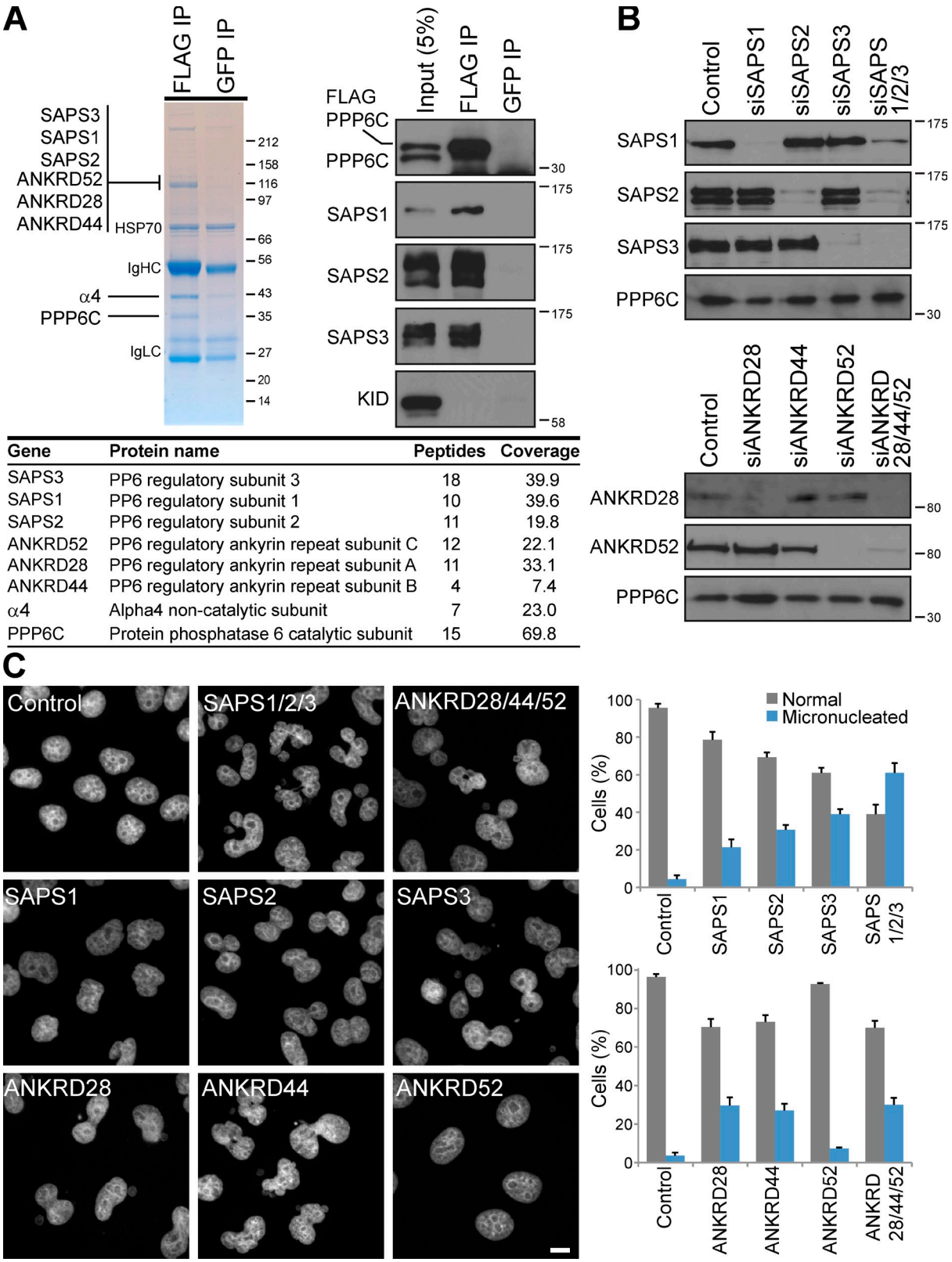

Gene	Protein name	Peptides	Coverage
SAPS3	PP6 regulatory subunit 3	18	39.9
SAPS1	PP6 regulatory subunit 1	10	39.6
SAPS2	PP6 regulatory subunit 2	11	19.8
ANKRD52	PP6 regulatory ankyrin repeat subunit C	12	22.1
ANKRD28	PP6 regulatory ankyrin repeat subunit A	11	33.1
ANKRD44	PP6 regulatory ankyrin repeat subunit B	4	7.4
α4	Alpha4 non-catalytic subunit	7	23.0
PPP6C	Protein phosphatase 6 catalytic subunit	15	69.8

Figure 2. **The PP6 holoenzyme is required for normal nuclear morphology.** (A) PP6 complexes were purified from a cell line stably expressing PPP6C tagged at the C terminus with a FLAG epitope. The cells were arrested in mitosis using 200 ng/ml nocodazole for 18 h before cell lysis. The complexes were analyzed by mass spectrometry, SDS-PAGE, and Western blotting. Sequence coverage is based on the total number of peptides matching the protein found using Mascot, whereas peptide number is the number of peptides reported to be unique to this protein by MaxQuant and is thus a more stringent measure of identification for closely related proteins. (B and C) HeLa cells were transfected with control, SAPS, and ankyrin repeat domain siRNA duplexes alone or in combination for 48 h. The cells were Western blotted to verify depletion of the target proteins (B) or fixed and then stained with DAPI (shown), tubulin, and CREST antibodies (C). The graph shows the percentages of normal and micronucleated cells for the various conditions ($n = 3$). Molecular mass is given in kilodaltons. Error bars indicate the standard error of the mean. IP, immunoprecipitation. Bar, 10 µm.

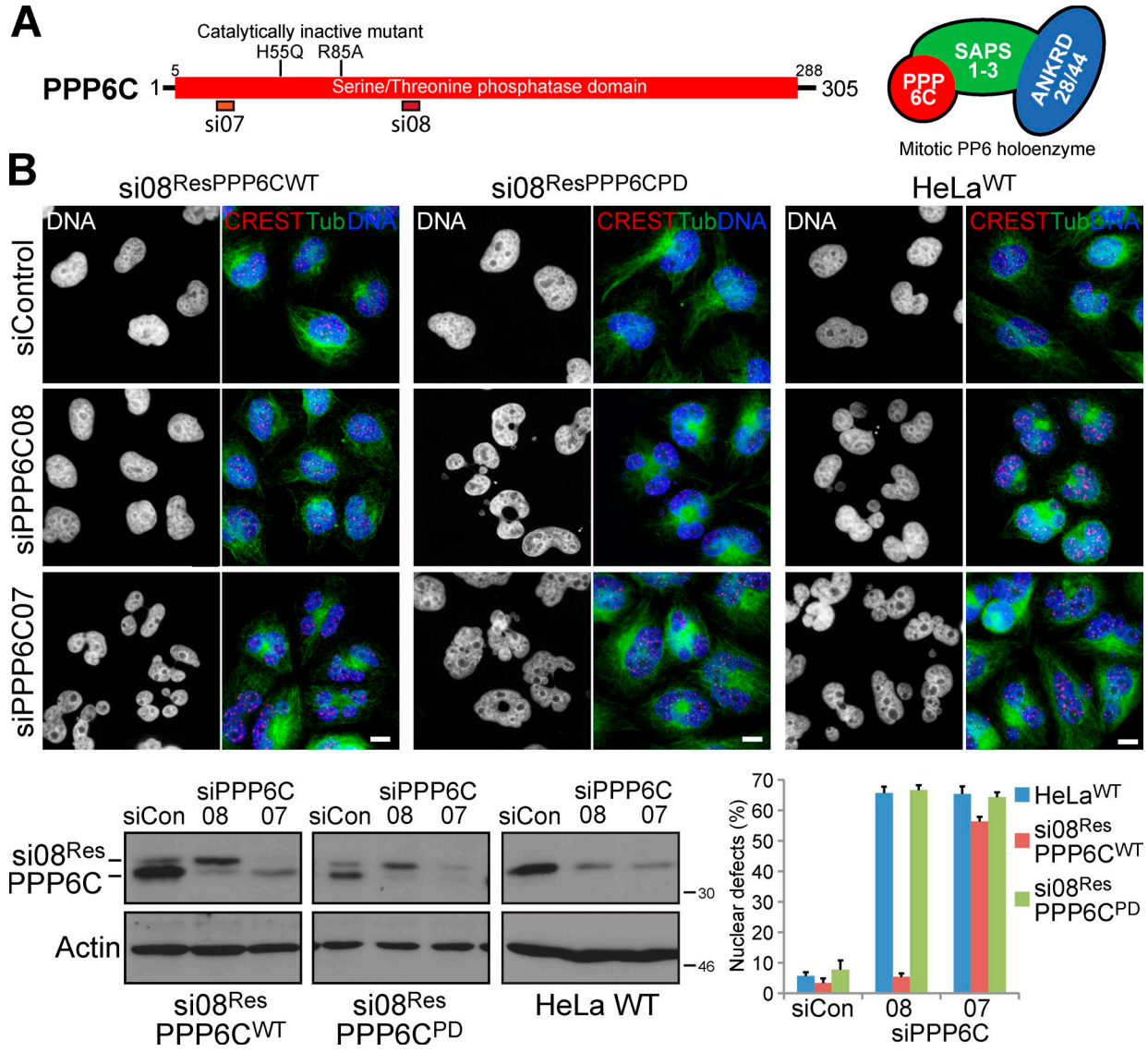

Figure 3. **PP6 catalytic activity is required for normal nuclear morphology.** (A) A schematic depicting the PP6 holoenzyme, PPP6C catalytic subunit, positions of siRNA duplexes used, and inactivating mutations. (B) HeLa cells stably expressing PPP6C si08–resistant wild-type (si08^{Res}PPP6C^{WT}) and phosphatase-dead mutant (si08^{Res}PPP6C^{PD}) forms of PPP6C tagged at the C terminus with a FLAG epitope were transfected with control (siCon) or si07 and si08 duplexes targeting PPP6C for 48 h. The cells were Western blotted or fixed and then stained with DAPI, tubulin (Tub), and CREST antibodies. Abnormal nuclear morphology was scored for each condition and is plotted in the graph (n = 3). Molecular mass is given in kilodaltons. Error bars indicate the standard error of the mean. Bars, 10 µm.

form by si07 alone was verified by Western blotting (Fig. 3 B). Interestingly, the levels of transgene-expressed PPP6C increased when the endogenous PPP6C was depleted with si08 (Fig. 3 B), suggesting that the availability of the PP6 regulatory and ankyrin repeat subunits may be limiting for PPP6C stability under these conditions.

PP6 is required for timely spindle formation

Although the visual screen for defective nuclear morphology implicates PP6 in mitotic progression, it does not define the process it functions in or, more importantly, what its substrates are. PP6 is localized to the cytoplasm (Fig. S2, A and B), giving little clue to its function. PPP6C depletion in either the HeLa cervical carcinoma cell line or MRC-5 human diploid lung fibroblasts caused similar patterns of altered nuclear morphology and the formation of micronuclei (Fig. 4, A–C). The micronuclei overlap with a single puncta of CREST centromeric marker autoantiserum staining (Fig. 4, A and B). This indicates that they correspond to single chromosomes, possibly arising through defects in chromosome segregation. To test whether the abnormal nuclei in PPP6C-depleted cells arise because of defective chromosome alignment and segregation, HeLa (Fig. 4 D) or MRC-5 (Fig. 4 E) cells were examined in mitosis. Control cells showed tightly aligned chromosomes in metaphase, which remain as well-defined masses as they segregate in anaphase and give rise to single nuclei in telophase (Fig. 4, D and E). In both cell lines tested, efficient PPP6C depletion resulted in poorly organized chromosome segregation in anaphase and in the formation of fragmented nuclei in telophase (Fig. 4, D and E). Similar effects

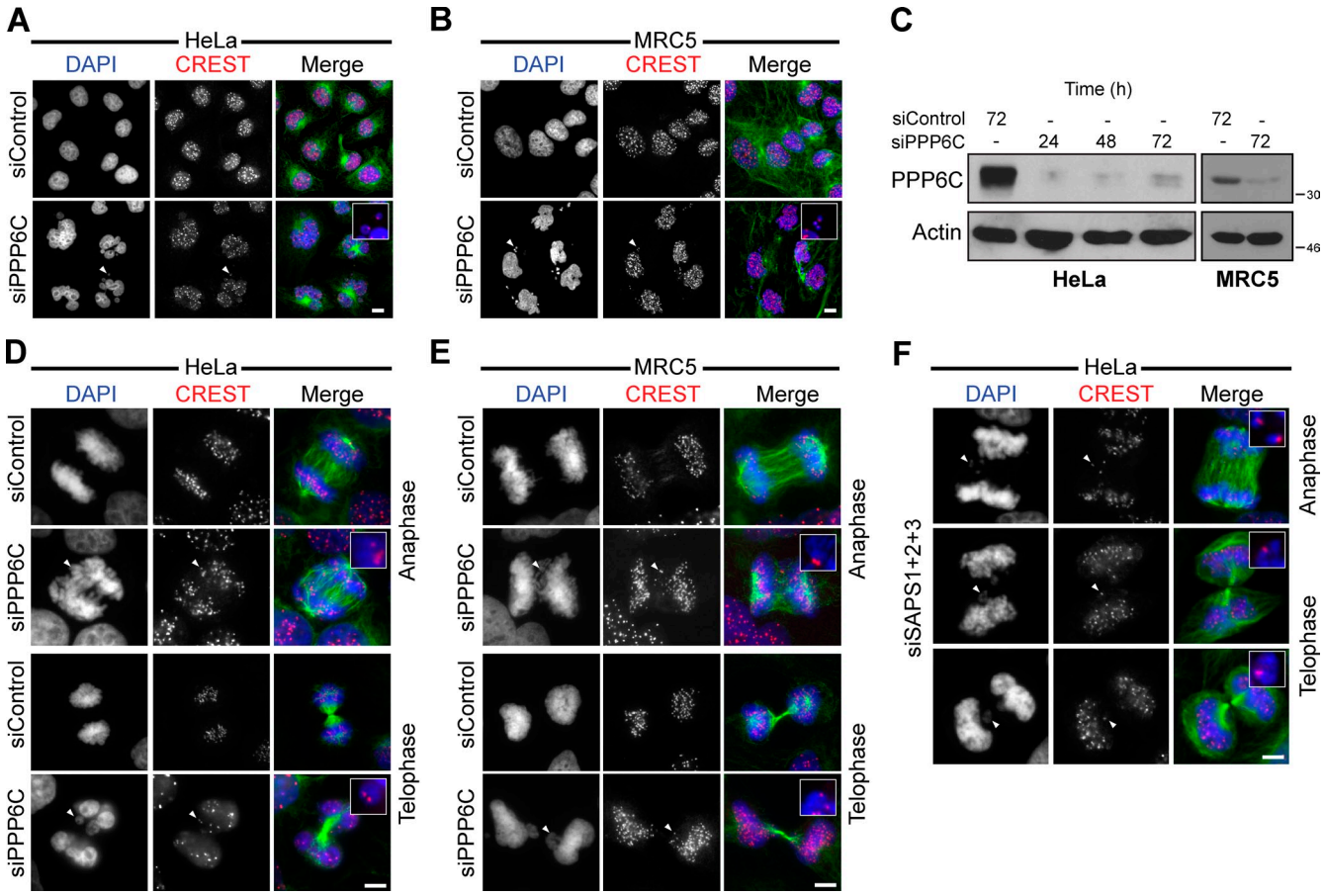

Figure 4. **Abnormal chromosome segregation in PPP6C-depleted cells.** (A and B) HeLa (A) and MRC-5 (B) cells were transfected with control and PPP6C siRNA duplexes for 24–72 h. The cells were fixed and then stained with DAPI, tubulin (green), and CREST antibodies. Bars, 10 µm. (C) The same samples were also Western blotted to test for PPP6C depletion. Molecular mass is given in kilodaltons. (D and E) Control and PPP6C-depleted HeLa (D) and MRC-5 (E) cells in anaphase and telophase are shown. (F) HeLa cells were transfected with all three SAPS domain siRNA duplexes for 72 h. The cells were fixed and then stained with DAPI, tubulin (green), and CREST antibodies. Cells in anaphase and telophase are shown. (D–F) Bars, 5 µm. In all panels, arrowheads mark lagging chromosomes, and these regions are shown in the inset enlargements.

were seen in cells depleted of all three SAPS domain proteins (Fig. 4 F). This supports the idea that the PP6 holoenzyme is required for normal mitotic progression. Live-cell imaging of cells stably expressing EGFP-tagged histone H2B (Fig. 5 A) or mCherry-tagged histone H2B and EGFP-tagged α-tubulin (Fig. 5 B) revealed that PPP6C-depleted cells did not form a bipolar spindle with normal kinetics and failed to efficiently align their chromosomes at the metaphase plate. These cells also showed a prolonged arrest in mitosis (Fig. 5, A–C), during which time the chromosomes continuously tumbled about before eventually aligning to form a loose metaphase plate (Fig. 5, A and B; Video 1 and Video 2 show control and PPP6C-depleted cells, respectively). After an extended period, PPP6C-depleted cells formed bipolar spindles (Fig. 5 B). However, these were disordered compared with control cells. Biochemical analysis of thymidine-synchronized cells depleted of PPP6C passing through mitosis revealed elevated levels of pT288-phosphorylated Aurora A and delayed passage through mitosis, as judged by the timing of cyclin B degradation (Fig. 5 D). These observations hinted at a defect in the pathway of spindle formation or chromosome capture. Examination of the PPP6C-depleted cells revealed no obvious changes in kinetochore or checkpoint proteins (Fig. S3 A). Cold-stable kinetochore fiber microtubule bundles, although disordered, were also still present in PPP6C-depleted cells but lost in Nuf2-depleted cells (Fig. S3 B), in which the kinetochore attachment site is disrupted (DeLuca et al., 2002). In contrast, the centrosomes defined by pericentrin often failed to localize at the spindle poles in PPP6C-depleted cells (Fig. S3, B and C). The defects in efficient chromosome capture and alignment seen in the absence of PP6 function do not appear to be caused by unstable kinetochore fibers or gross kinetochore defects and could therefore be caused by misregulation of the centrosome-mediated spindle formation pathway.

PP6 is an Aurora A T-loop phosphatase

To pursue the idea that PP6 is a mitotic regulator important for spindle formation, stage 2 of the screen was focused on the key kinase regulators of spindle formation from the centrosome Aurora A and Plk1 (Llamazares et al., 1991; Glover et al., 1995; Lane and Nigg, 1996; Roghi et al., 1998). If the T-loop phosphatase acting on either kinase is absent, the phosphorylated form will be stabilized under conditions in which dephosphorylation is normally favored over phosphorylation (Ahonen et al., 2005; Daum and Gorbsky, 2006). This can be simply achieved

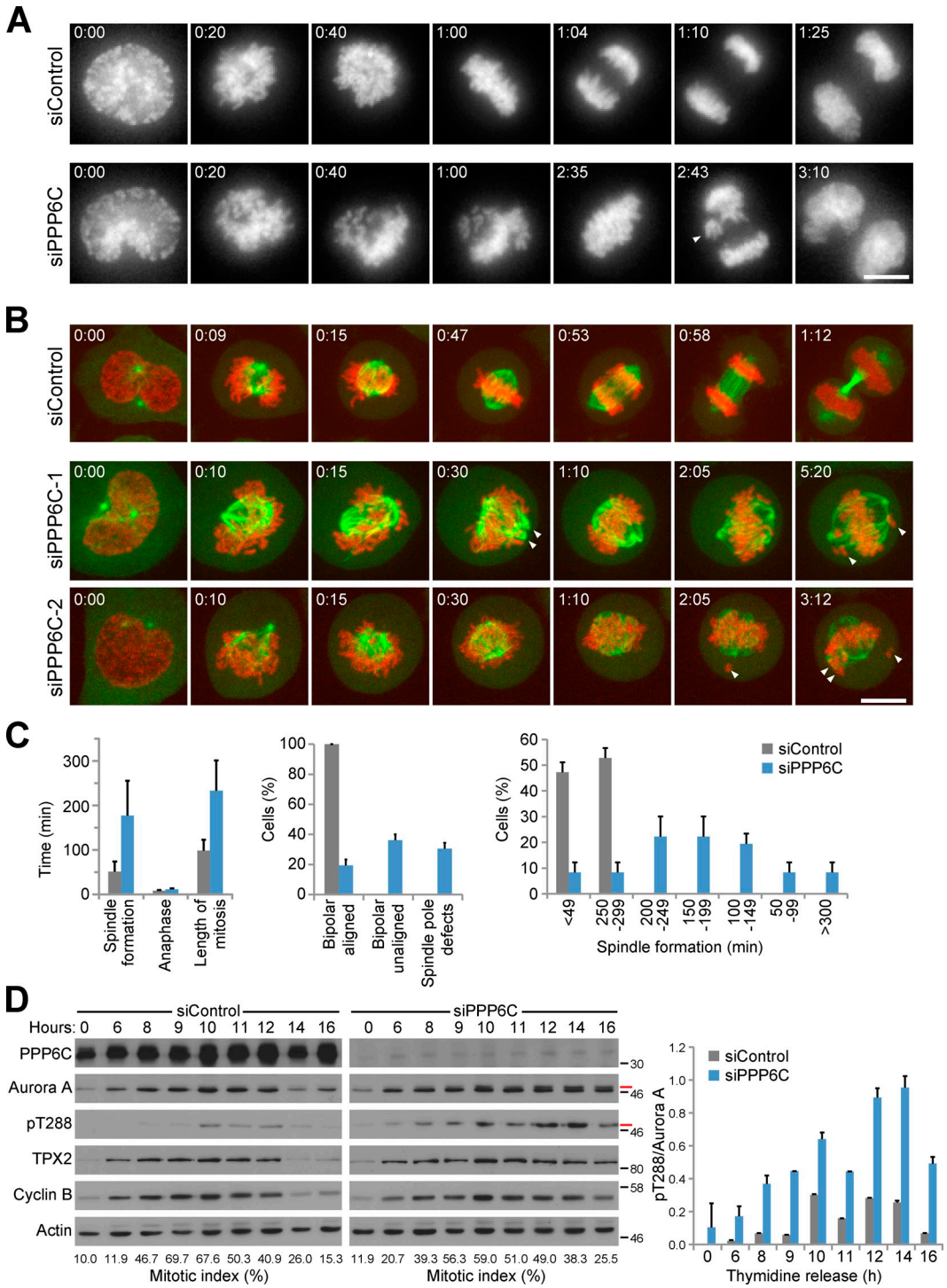

Figure 5. **Abnormal spindle formation in PPP6C-depleted cells.** (A) HeLa cells stably expressing EGFP-tagged histone H2B were transfected with control or PPP6C si08 duplexes for 48 h and then imaged. An image stack of 25 planes spaced 0.7 µm apart was taken at four stage positions every minute for 10–12 h. Exposure times were 10 ms for EGFP-tagged histone H2B using 1% of full lamp intensity. A brightfield reference image stack was also collected using 10-ms exposures. (B) HeLa cells stably expressing mCherry-tagged histone H2B and EGFP-tagged α-tubulin were transfected for 48 h with control or PPP6C si08 duplexes and then imaged every minute at three stage positions for 10 h using a spinning-disk confocal microscope (Ultraview Vox). Laser settings were 3% with 30-ms exposure per channel, and 35 optical sections spaced 0.5 µm apart were taken for both channels. Representative examples of cells passing through mitosis are shown. The times are given in hours and minutes. Arrowheads mark abnormal spindle poles and lagging chromosomes. (C) The time taken to form a spindle and pass through mitosis was measured from the live-cell imaging and is plotted in the graphs (40 cells from three experiments). A histogram of spindle formation is also shown with a graph showing the observed defects in chromosome alignment and spindle poles (38 cells from three experiments). (D) HeLa cells were transfected with control or PPP6C si08 duplexes for 48 h. During the last 18 h, they were arrested with 2 mM thymidine. After washout of the thymidine, samples were collected at the times indicated, split, and used for FACS analysis or Western blotting. Mitotic index calculated from the FACS analysis is shown below the Western blot at the corresponding time point. The graph shows the ratio of phosphorylated/total Aurora A at each time point (n = 2). Where present, the red and black lines indicate the phosphorylated and nonphosphorylated forms of Aurora A. Molecular mass is given in kilodaltons. Error bars indicate the standard error of the mean. Bars, 10 µm.

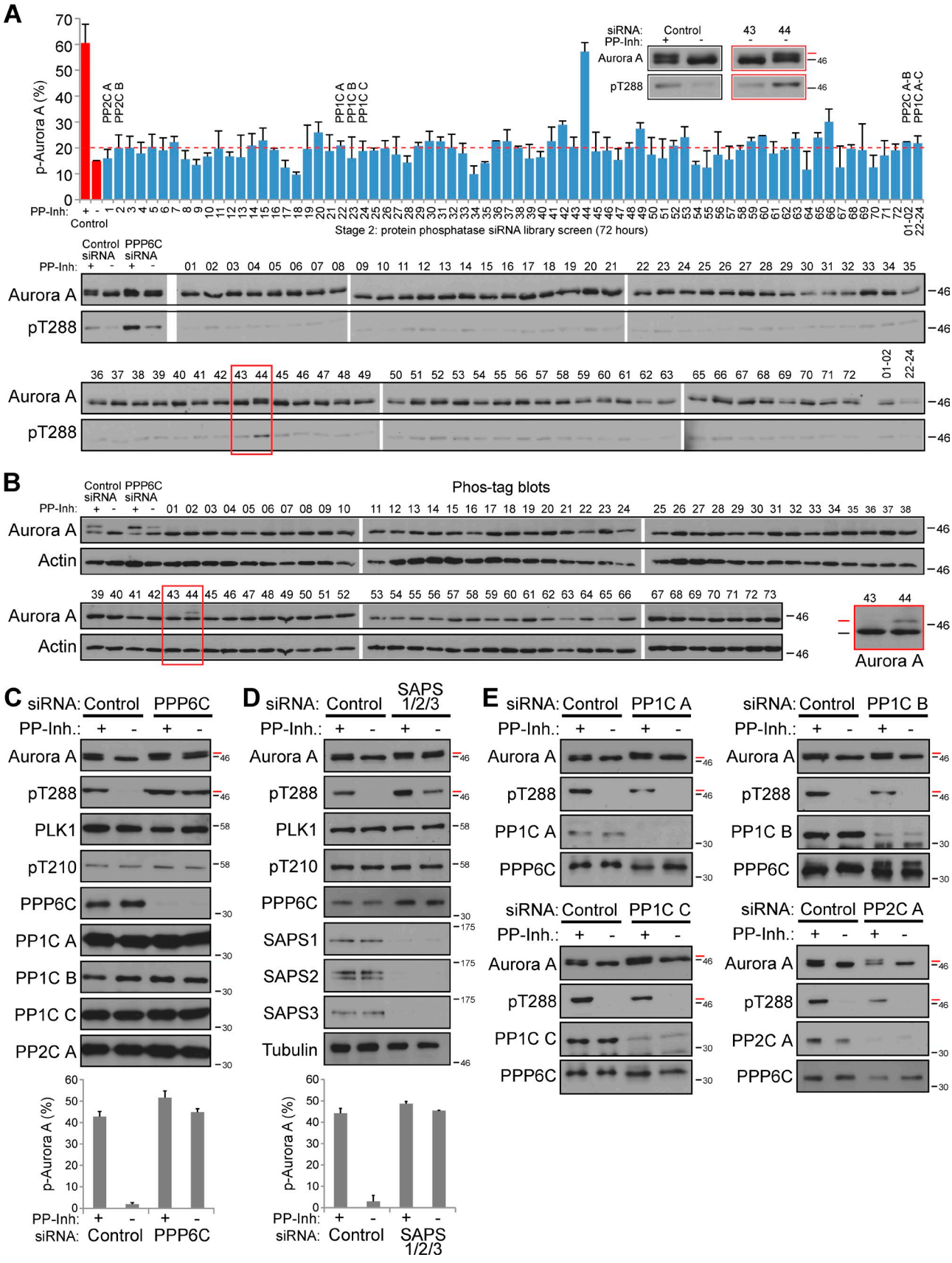

Figure 6. **Identification of PP6 as the Aurora A T-loop phosphatase.** (A) HeLa cells were transfected with siRNA pools for 72 human phosphatase subunits for 54 h, treated for 18 h with nocodazole, and then lysed in the absence of phosphatase inhibitors for 2 h on ice. Control samples were lysed in the presence or absence of phosphatase inhibitors (PP-Inh). Samples were Western blotted for total Aurora A and Aurora A pT288. The graph shows the ratio of

by cell lysis on ice for 2 h in the absence of phosphatase inhibitors (outlined in Fig. 1 B, stage 2).

Cell lysates prepared from control or phosphatase subunit–depleted cells were therefore Western blotted with antibodies to Aurora A and the phosphorylated T288 T-loop residue (Ohashi et al., 2006). Because the visual screen indicated some redundancy between PP1 and PP2 catalytic subunits, these were depleted alone and in combination. As expected, Aurora A phosphorylation was lost during lysate preparation from control cells using standard lysis procedures without phosphatase inhibitors (Fig. 6 A, red bars). Notably, it was retained in PPP6C-depleted cell lysates but not under the other conditions tested (Fig. 6 A, duplex 44), suggesting that PP6 is the major Aurora A T-loop phosphatase. This shift was more clearly seen on gels cast with the Phos-tag reagent (Fig. 6 B, duplex 44), which slows the mobility of phosphorylated proteins and, thus, better resolves them from their nonphosphorylated counterpart. Several criteria suggest that Aurora A is a specific target of PP6. No other phosphatase tested stabilized the phosphorylated form of Aurora A (Fig. 6, A and B). Both the Aurora A pT288 signal and the upshifted phosphorylated form of Aurora A were protected after depletion of either the PP6 catalytic or SAPS regulatory subunits (Fig. 6, C and D, respectively), which was consistent with a requirement for the PP6 holoenzyme. Plk1 is phosphorylated on T210 (Jang et al., 2002), and, in contrast to Aurora A T288 phosphorylation, this was not altered by PP6 catalytic or SAPS regulatory subunit depletion (Fig. 6, C and D). Levels of other phosphatases, such as PP1 and PP2, were unaltered under these conditions (Fig. 6 C), suggesting altered Aurora A phosphorylation was primarily caused by the loss of PP6 activity. Addition of excess phosphatase inhibitor cocktail to the buffer stabilized Aurora A T288 phosphorylation and the upshifted form of Aurora A and revealed that there is slightly more T288-phosphorylated Aurora A in PP6 catalytic or regulatory subunit–depleted cells than in the control cells (Fig. 6, C and D). Depletion of the PP1 and PP2 catalytic subunits alone (Fig. 6 E) or in combination (Fig. 6 A) did not stabilize Aurora A phosphorylation. Together, these observations indicate that the PP6 holoenzyme comprising both catalytic and regulatory subunits is an Aurora A T-loop phosphatase and that the underlying defect after the loss of PP6 function is misregulation of Aurora A and not Plk1.

PP6 acts on the Aurora A–TPX2 complex

Activated Aurora A forms a complex with the spindle assembly factor TPX2 (Kufer et al., 2002; Bayliss et al., 2003; Eyers and Maller, 2004), and the effects of PP6 inactivation on the Aurora A–TPX2 complex were therefore investigated. As already shown, standard lysis procedures resulted in the loss of Aurora A phosphorylation in control cell lysates (Fig. 7 A, lanes 1–4). Consistent with this, TPX2 did not interact with Aurora A under these conditions (Fig. 7 A, lane 6). Depletion of the PP6 catalytic subunit using si08 or the addition of excess phosphatase inhibitors stabilized the upshifted form of Aurora A and its interaction with TPX2 (Fig. 7 A, compare lanes 8 and 9 with lanes 5 and 6). Kinase assays on these complexes showed that PPP6C depletion stabilized Aurora A kinase activity toward TPX2 and the model substrate histone H3 under conditions in which it is lost in the control samples (Fig. 7 A, compare lane 9 with lane 6). Similarly, depletion of PPP6C using a second duplex, si07, or of the PP6 SAPS1/2/3 regulatory subunits stabilized the upshifted form of Aurora A and its interaction with TPX2 (Fig. 7 B, compare lanes 7 and 8 with lanes 10 and 11 and 13 and 14). In contrast, depletion of PP2A or PP1 catalytic subunits did not stabilize either the upshifted pool of Aurora A or its interaction with TPX2 (Fig. 7, C and D, compare lanes 7 and 8 or 20 and 21 with lanes 10 and 11, 13 and 14, and 23 and 24). This is in agreement with previous findings that these phosphatases can only act on free Aurora A and not Aurora A in complex with TPX2 (Bayliss et al., 2003; Eyers et al., 2003).

To provide further evidence that PP6 acts directly on Aurora A–TPX2 complexes, phosphatase assays using purified proteins were performed. When Aurora A–TPX2 complexes were incubated with the catalytically active PP6 holoenzyme purified from mitotic cells, Aurora A was dephosphorylated (Fig. 7 E, lane 2). This effect was not seen when buffer, catalytically inactive PP6, or a mock enzyme purification was used (Fig. 7 E, lanes 1, 3, and 4). The nonspecific phosphatase activity of calf intestinal phosphatase was unable to dephosphorylate Aurora A–TPX2 complexes under these conditions (Fig. 7 E, lane 5), which was consistent with previous observations that the phosphorylated T288 T-loop residue is protected in the TPX2 complex. This suggests that PP6 specifically recognizes the Aurora A–TPX2 complex and gains access to the protected phosphorylated T288 residue (Bayliss et al., 2003). These observations are summarized in a model in which the PP6 holoenzyme acts on the Aurora A–TPX2 complex, whereas PP1 and PP2A act on free Aurora A (Fig. 7 F).

Aurora A inhibition rescues the PPP6C depletion phenotype

Previous studies have suggested that activated Aurora A in complex with TPX2 accumulates at the spindle (Kufer et al., 2002; Bayliss et al., 2003; Eyers et al., 2003; Ozlü et al., 2005; Ohashi et al., 2006). Loss of PP6 function, which stabilizes the Aurora A–TPX2 complex, should, therefore, result in increased levels of

phosphorylated/total Aurora A (n = 2). The red line indicates the median value for Aurora A phosphorylation. (B) HeLa cells were transfected with siRNA pools for 73 human phosphatase subunits for 54 h, treated for 18 h with nocodazole, and then lysed in the absence of phosphatase inhibitors for 2 h on ice. In addition, control and PPP6C-depleted samples were lysed in the presence or absence of phosphatase inhibitors. All samples were analyzed on Mn^{2+} Phos-tag gels to better resolve phosphorylated from nonphosphorylated Aurora A and then Western blotted for total Aurora A and actin as a loading control. Red boxes highlight siRNA 44 (PPP6C) in which Aurora A phosphorylation is retained and an adjacent sample in which it is not. (C–E) HeLa cells were transfected for 48 h with control, PPP6C si08, SAPS1–3, PP1C A, PP1C B, PP1C C, and PP2C A siRNA duplexes. Lysates were then prepared from these cells in immunoprecipitation buffer containing or lacking phosphatase inhibitor cocktail and Western blotted. Graphs show phosphorylated Aurora A levels (n = 3). Molecular mass is given in kilodaltons. Error bars indicate the standard error of the mean. Where present, the red and black lines indicate the phosphorylated and nonphosphorylated forms of Aurora A. White lines indicate that intervening lanes have been spliced out.

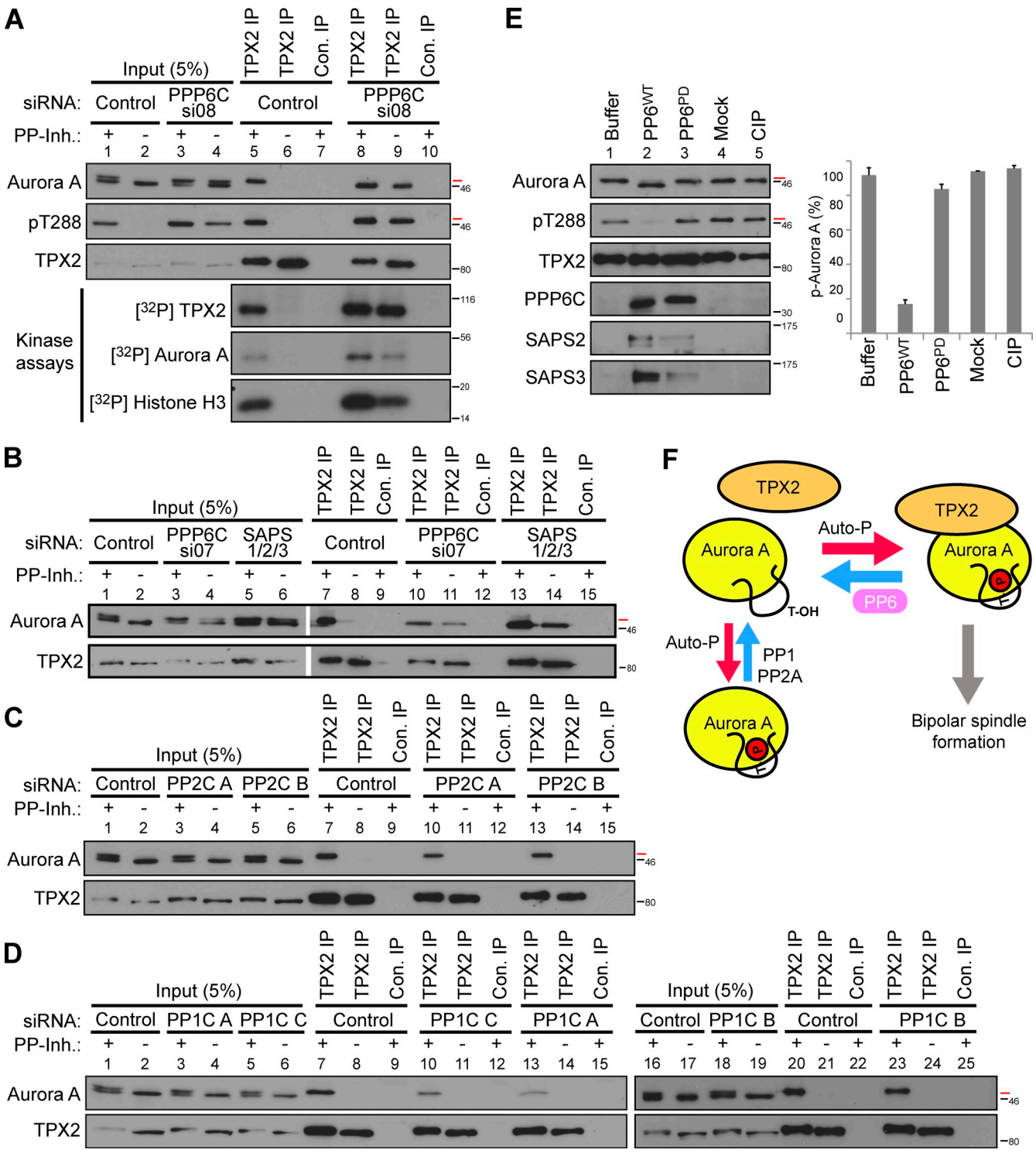

Figure 7. **PP6 catalytic or regulatory subunit depletion stabilizes the Aurora A–TPX2 complex.** (A and B) TPX2–Aurora A complexes were isolated from control and PPP6C si08 (A) or control, PPP6C si07, or SAPS1–3-depleted (B) cell lysates prepared in the presence or absence of phosphatase inhibitors (PP-Inh.). GFP antibodies were used as a negative control (Con.). Total lysates and immune-precipitated (IP) material were Western blotted or used for kinase assays as indicated. White lines indicate that intervening lanes have been spliced out. (C and D) TPX2–Aurora A complexes were isolated from control, PP2C A–, and PP2C B–depleted (C) or control and PP1C A–, B–, and C–depleted (D) cell lysates prepared in the presence or absence of phosphatase inhibitors. Total lysates and immune-precipitated material were Western blotted. (E) Purified Aurora A–TPX2 complexes were incubated with wild-type or catalytically inactive recombinant PP6 holoenzymes, $PP6^{WT}$ and $PP6^{PD}$, respectively, buffer, mock-purified enzyme, or 2.5 U of calf intestinal phosphatase (CIP) for 2 h and then Western blotted. The graph shows phosphorylated Aurora A levels ($n = 2$). Error bars indicate the standard error of the mean. (F) A model outlining the role of PP6 as an Aurora A–TPX2 phosphatase. PP1 and PP2A can act as free Aurora A phosphatases but cannot recognize the TPX2-complexed form that promotes spindle formation. Where present, the red and black lines indicate the phosphorylated and nonphosphorylated forms of Aurora A. Molecular mass is given in kilodaltons.

activated Aurora A at the mitotic spindle. Consistent with the biochemical changes, PPP6C-depleted cells showed altered staining at the spindle for activated Aurora A pT288 and the Aurora A activator TPX2 (Fig. S4, siPPP6C, arrowheads). In control cells, activated Aurora A pT288 and TPX2 staining was most predominant at the spindle poles with a faint staining spread along spindle microtubules (Fig. 8 A and Fig. S4, siControl). In PPP6C-depleted cells, the spindle microtubule staining of both activated Aurora A and TPX2 was increased (Fig. 8 A and Fig. S4, siPPP6C), and this could be reversed by a combined PPP6C and TPX2 depletion (Fig. S4, siPPP6C + TPX2). It was not possible to completely deplete TPX2, and a small amount always remained at centrosomes, where it overlapped with a population of activated Aurora A that was unaltered by PPP6C depletion.

Highly specific small molecule inhibitors for Aurora family kinases have recently been developed (Manfredi et al., 2007; Karthigeyan et al., 2010), and this suggested a rescue strategy for the PPP6C depletion phenotype. Low doses of Aurora A inhibitors were therefore tested to see whether they reversed the increased Aurora A activation and T-loop phosphorylation seen upon PPP6C depletion. Limiting titration of the Aurora A inhibitor MLN8237 did not block cell growth but reversed the effect of PPP6C depletion on Aurora A T-loop phosphorylation, with 10 nM MLN8237 resulting in the same ratio of activated to inactivated Aurora A seen in control cells in the absence of the drug (Fig. 8 A, gel image on bottom). Depletion of PPP6C resulted in a twofold increase in the pT288 form of Aurora A at prometaphase and metaphase spindles compared with control cells, and addition of 10 nM MLN8237 reversed this increase (Fig. 8 A). Importantly, this partial Aurora A inhibition with 10 nM MLN8237 also reduced the micronucleation seen in PPP6C-depleted cells from 40 to 5% (Fig. 8 B). Reduction of Aurora A activity using TPX2 depletion also rescued the PPP6C depletion nuclear morphology defect (Fig. 8 C), which was consistent with the idea that TPX2 and PP6 have opposing effects on Aurora A activity. These results suggest that PPP6C depletion results in unchecked activation of Aurora A caused by loss of the T-loop phosphatase activity and, thus, disturbs the fine balance of Aurora A–TPX2 complexes at the spindle required for chromosome capture and alignment. The reversal of the PPP6C phenotype by reduction of Aurora A activity using TPX2 depletion or MLN8237 also indicates that Aurora A is a major substrate of PP6.

PP6 opposes Aurora A to control spindle formation

Aurora A, together with the Ran–importin pathway, is part of a complex regulatory system controlling the action of spindle assembly factors, such as NuMa and TACC, and kinesin motor proteins, such as Eg5/KIF11, required to form a bipolar mitotic spindle (Giet et al., 1999, 2002; Tsai et al., 2003; Clarke and Zhang, 2008). The effect of PP6 inactivation by PPP6C depletion on these spindle assembly factors was therefore investigated. In control cells undergoing unperturbed mitosis, Eg5 and NuMa were recruited to the forming spindle poles in prophase and remained there until the onset of anaphase (Fig. 9 A, siControl). In contrast, cells depleted of PPP6C failed to recruit Eg5 and NuMa to spindle poles in prophase (Fig. 9 A, siPPP6C). Prometaphase spindle poles were also highly fragmented and disordered (Fig. 9 A, siPPP6C), which was consistent with the results obtained by live-cell imaging, which showed delayed spindle formation and defective spindle integrity (Fig. 5 B). To allow a better measurement of this effect, cells were arrested in prometaphase using the Eg5 inhibitor S-trityl-L-cysteine, and bipolar spindle formation followed after washout of the drug. In this assay, control cells rapidly formed a bipolar spindle within 15 min of drug washout, aligned their chromosomes, and entered anaphase by 60 min (Fig. 10, A and B). In contrast, PPP6C-depleted cells had a pronounced delay in both bipolar spindle formation and chromosome alignment (Fig. 10, A and B). This suggested that the spindle-associated activity of Eg5 and other spindle assembly factors may be limiting in PPP6C-depleted cells. In accordance with this idea, the spindle-associated level of both Eg5 and NuMa was reduced compared with control cells (Fig. 9 A and measured in Fig. S5). If this reduction was caused by unchecked Aurora A activity, Aurora A inhibition should reverse this effect. When PPP6C-depleted cells were treated with MLN8237 for 10 min to inhibit Aurora A, Eg5 localization to the spindle recovered to the levels seen in control cells, and focused NuMa staining around the spindle poles was reinstated (Fig. 9 B, compare siPPP6C with siPPP6C + 10 µM MLN8237 conditions). Collectively, these findings support a model in which PP6 regulates spindle formation by limiting the activity of the Aurora A–TPX2 complex toward key spindle assembly factors, including Eg5 and NuMa.

Discussion

PP6 is the Aurora A T-loop phosphatase

The findings reported here suggest that PP6 plays an important role during mitotic spindle formation. Specifically, PP6 is the T-loop phosphatase regulating Aurora A activity at the mitotic spindle. This may explain recent findings in *C. elegans* in which mutations in PP6 were found to cause mitotic defects in spindle positioning and cortical contractility of the early embryo (Afshar et al., 2010). These findings add to the previously reported functions of PP6 in S phase and nuclear factor–κB signaling (Stefansson and Brautigan, 2006; Mi et al., 2009; Douglas et al., 2010) and negative regulation of the Mis12 kinetochore protein in fission yeast (Goshima et al., 2003). Other PPP family phosphatases have many functions at different stages of the cell cycle and in a variety of processes in nondividing cells, which can be explained by their many different isoforms comprised of a series of closely related subunits. It is reasonable to believe that this is also true for PP6 (Stefansson et al., 2008) and that specific isoforms are likely to have functions in S phase and M phase. The results presented here suggest that the ANKRD28 and 44 subunits are required for PP6 function in mitosis, whereas ANKRD52 is not. Interestingly, ANKRD28 and 44 are most closely related, whereas ANKRD52 is less similar. This is intriguing because the MYPT1 ankyrin repeat subunit of PP1 is important in substrate recognition (Tóth et al., 2000; Terrak et al., 2004). Therefore, the forms of PP6 important in mitosis

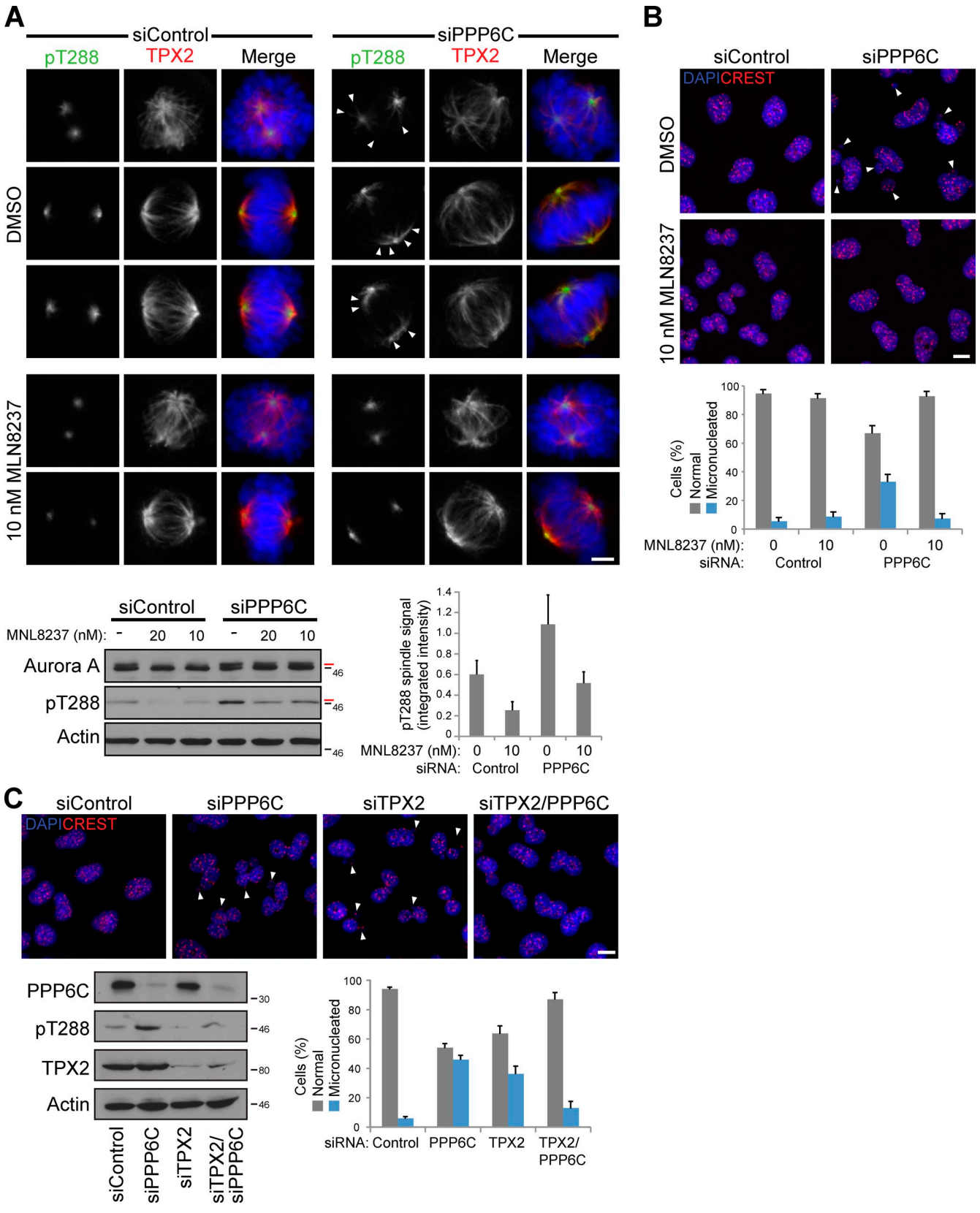

Figure 8. **Aurora A inhibition rescues the PPP6C depletion phenotype.** (A) HeLa cells transfected for 48 h with control and PPP6C si08 duplexes were treated with 10 or 20 nM MLN8237 or a solvent control for 15 min before lysis in phosphatase inhibitor containing buffer or fixation. Total lysates were analyzed by Western blotting. The red and black lines indicate the phosphorylated and nonphosphorylated forms of Aurora A. Fixed cells were stained using DAPI to detect DNA and antibodies to α-tubulin and Aurora A pT288. The intensity of pT288 staining was integrated using ImageJ over the spindle region defined by TPX2 staining and is plotted in the bar graph ($n = 4$). Arrowheads indicate micronuclei. Bar, 5 µm. (B) HeLa cells transfected for 48 h with control and PPP6C si08 duplexes were treated with 10 nM MLN8237 or a solvent control for 24 h before fixation and staining with DAPI to detect DNA

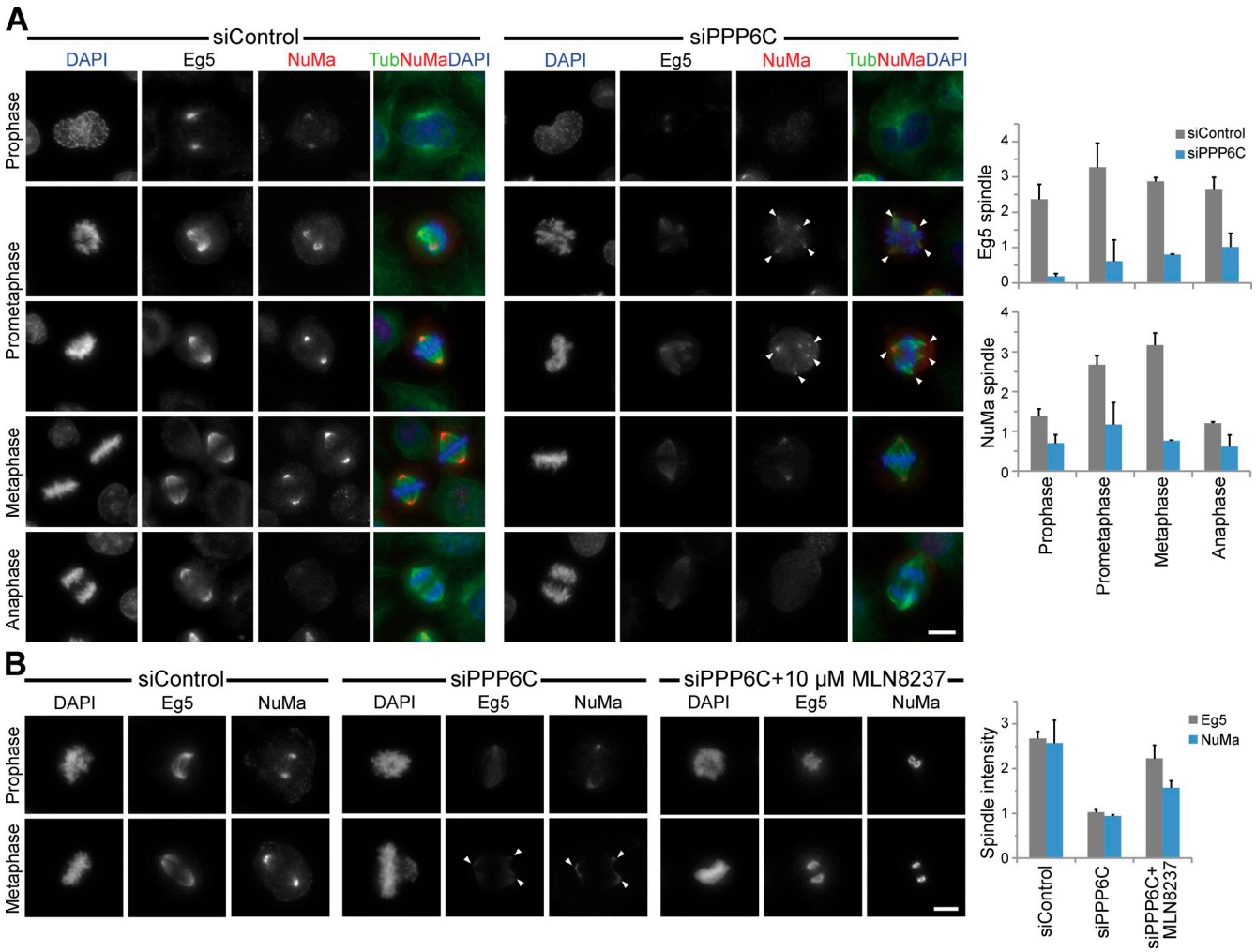

Figure 9. **Spindle assembly factors are misregulated after PPP6C depletion.** (A) HeLa cells were transfected for 48 h with control or PPP6C si08 duplexes before fixation. Cells were stained using DAPI to detect DNA and antibodies to α-tubulin (Tub), Eg5, and NuMa. (B) Control and PPP6C-depleted cells treated with solvent (DMSO) or 10 μM MLN8237 for 10 min were fixed and then stained for Eg5, NuMa, tubulin (not depicted), and with DAPI to detect DNA. Bars, 10 μm. In both panels, KIF11/Eg5, NuMa, and tubulin signals were measured for the spindle region in ImageJ. KIF11/Eg5 and NuMa signals were normalized for tubulin and are plotted in the graph (n = 12). Error bars indicate the standard error of the mean. Arrowheads mark fragmented spindle poles.

and S phase may have unique substrates determined by the ANKRD28/44 and 52 subunits, and this will be an important avenue for further investigation.

Exactly what constitutes a PP6 substrate recognition determinant is unclear. In the future, it should be possible to define this determinant by comparing the mitotic PP6 substrate Aurora A and the closely related kinase Aurora B, which is not a substrate (unpublished data). High quality crystal structures have been solved for both the Aurora A–TPX2 and the Aurora B–INCENP (inner centromere protein) complexes (Bayliss et al., 2003; Sessa et al., 2005). These reveal that Aurora A pT288 is exposed to solvent in the absence of TPX2, reorients and hydrogen bonds with Aurora A–arginine 255, and, thus, is protected from the bulk solution in the presence of TPX2. Here, we show that PP6 is a physiologically relevant T-loop phosphatase in human cells, which recognizes the active, TPX2-complexed form of Aurora A. This suggests that PP6 can access the buried pT288 residue, possibly by altering the conformation of the Aurora A–TPX2 complex. An intriguing possibility is that the Aurora A–specific activator TPX2 also acts as a recognition determinant for the PP6 T-loop phosphatase. This would allow PP6 to specifically recognize and act upon the Aurora A–TPX2 complex.

Previous studies have reported that Aurora A can be dephosphorylated by PP1 or PP2A in vitro (Andrésson and Ruderman, 1998; Walter et al., 2000; Bayliss et al., 2003; Eyers et al., 2003; Tsai et al., 2003). However, this is prevented in the

and CREST to mark centromeres. Micronucleation is quantitated in the graph (n = 3). (C) HeLa cells were transfected for 48 h with control, PPP6C si08, and TPX2 duplexes alone or in combination before fixation. Cells were stained using DAPI to detect DNA and CREST to mark centromeres. The graph shows the percentages of normal and micronucleated cells for the various conditions (n = 3). (B and C) Arrowheads indicate CREST staining outside the main nucleus defined by the DAPI staining. Bars, 10 μm. Molecular mass is given in kilodaltons. Error bars indicate the standard error of the mean.

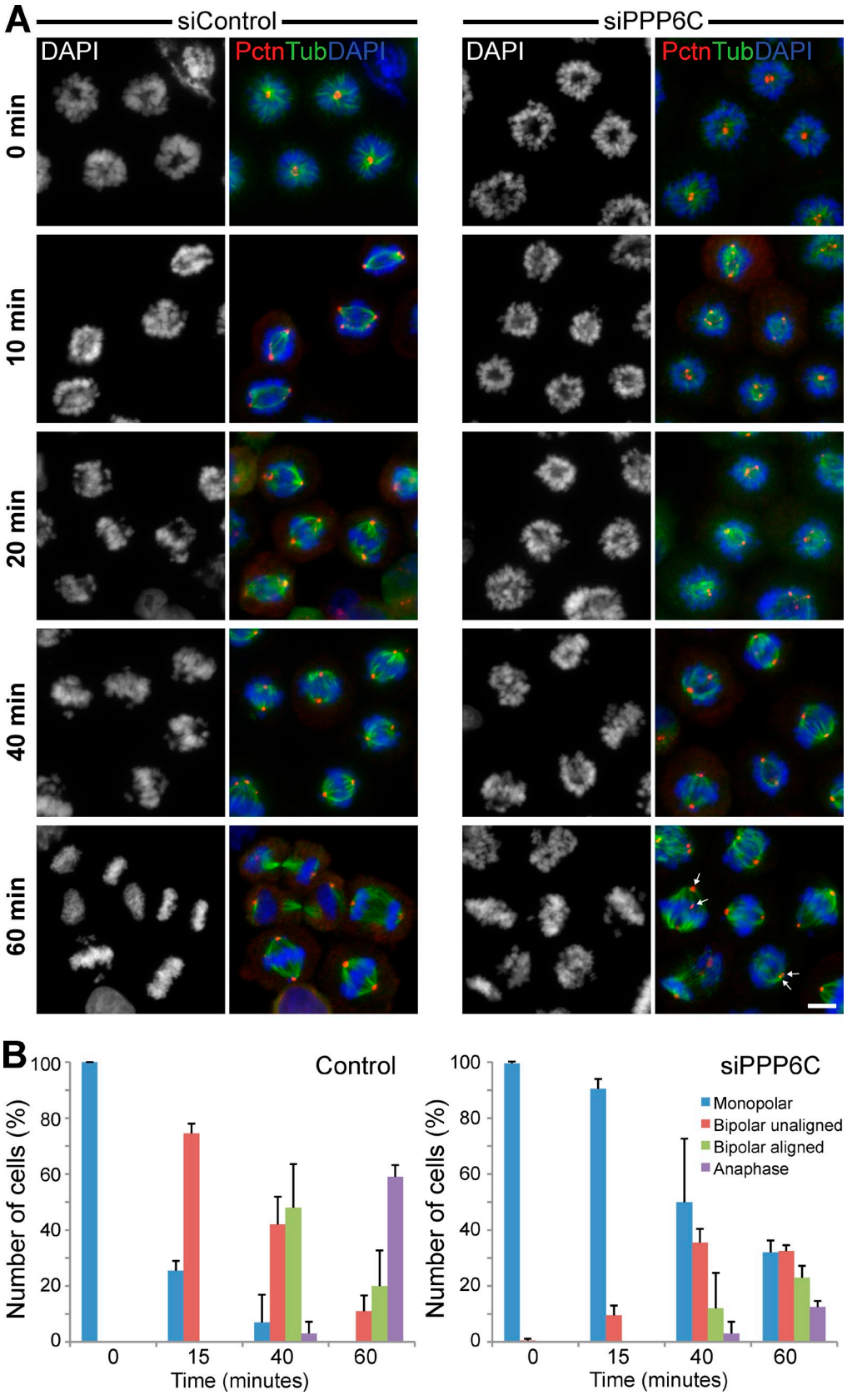

Figure 10. **Bipolar spindle formation is delayed in PPP6C-depleted cells.** (A) HeLa cells were transfected with control and PPP6C siRNA duplexes for 48 h and then arrested overnight with S-trityl-L-cysteine to inhibit Eg5. The drug was washed out with fresh medium, and the cells were fixed at the time points indicated. Cells were stained with DAPI, tubulin (Tub), and pericentrin (Pctn) antibodies. Arrows mark the positions of pericentrin-positive centriole structures. Bar, 10 µm. (B) The spindle and chromosome alignment status of control and PPP6C-depleted cells was counted at the times indicated and is plotted in the graph (n = 4). Error bars indicate the standard error of the mean.

Aurora A–TPX2 complex (Bayliss et al., 2003; Eyers et al., 2003; Tsai et al., 2003), and, paradoxically, PP1 is therefore unable to act upon the active form of Aurora A. As shown here, PP6 is able to act on the Aurora A–TPX2 complex and does not suffer this limitation. PP6 is also the major Aurora A T-loop phosphatase activity in cell lysates, and PP1 contributes little, if any, activity consistent with the finding that PP1 is inactivated by inhibitory CDK1 phosphorylations in mitosis (Dohadwala, 1994; Kwon, 1997). This raises the question of how PP6 has been overlooked until now. There may be three reasons for this. First, PP6 is inhibited by the toxins okadaic acid, microcystin-LR, and calyculin A used to study PP1 and PP2A, and, depending on the model substrate used, is actually more sensitive than PP2A to these toxins (Prickett and Brautigan, 2006). In fact, the residues in PP2A required for very high affinity toxin binding are conserved in PP6, including the hydrophobic cage–forming residues glutamine 122 and histidine 191 (Xing et al., 2006). These residues are not conserved in PP1, explaining the reduced inhibition of PP1 by okadaic acid and microcystin-LR (Xing et al., 2006). Therefore, inhibitor studies do not unambiguously define which PPP family member is acting on a specific target. Second, inhibitor-2 (I-2) was previously used to implicate PP1 as the Aurora A phosphatase (Tsai et al., 2003). However, it was subsequently shown that I-2 can directly stimulate Aurora A autophosphorylation activity (Satinover et al., 2004), suggesting that the effects of I-2 are independent of any inhibition of PP1. Third, previous studies have used the commercially available trypsin-resistant catalytic fragment of PP1, which lacks the regulatory subunits and, therefore, does not have the same substrate specificity as the PP1 holoenzyme (Johnson et al., 1987; Tóth et al., 2000; Terrak et al., 2004). The high degree of similarity in PPP family catalytic subunits also means that in the absence of regulatory subunits they will have limited specificity (Xing et al., 2006). Fitting with this view, catalytic subunits alone of either PP1 or PP2A can dephosphorylate free Aurora A (Bayliss et al., 2003; Eyers et al., 2003; Tsai et al., 2003).

Aurora A and PP6 in cancer

Finally, our findings have relevance beyond the biochemistry and cell biology of Aurora A regulation. Aurora A is amplified in many cancers and is currently the focus of much interest as a drug target for cancer therapy (Sen et al., 1997; Bischoff et al., 1998; Zhou et al., 1998; Karthigeyan et al., 2010). Intriguingly, PPP6C is mutated at an absolutely conserved histidine lying within the catalytic site in melanoma (Bamford et al., 2004; Forbes et al., 2010). As we show here, loss of PP6 function will lead to increased Aurora A activity similar to the effects of Aurora A amplification. PPP6C could therefore be considered a novel tumor suppressor gene. Recent work suggests that the mitotic machinery is an Achilles' heel for cancer cells carrying mutant Ras (Luo et al., 2009), and innovative ways of targeting key mitotic regulators are therefore of great interest. Our work suggests additional ways in which Aurora A activity can be targeted through inactivation of PP6. PP6 inhibitors may be useful for targeting cancers with amplified or in some other way perturbed Aurora A activity. Under these conditions, PP6 inhibition might push the system into a runaway state that directly promotes cell death or sensitizes the cells to other mitotic poisons. Further work will be necessary to test these ideas, but preliminary data support this hypothesis (unpublished data). The strategy presented here is also likely to have general relevance for other classes of enzyme important for cell cycle control and cell signaling pathways. Although it is notoriously difficult to identify enzyme substrates, the biochemical method used here provides a simple way to find the specific enzyme-catalyzing removal of any labile modification, such as phosphorylation, ubiquitylation, sumoylation, and others.

Materials and methods

Reagents and antibodies

Standard laboratory reagents were obtained from Thermo Fisher Scientific and Sigma-Aldrich. Antibodies to Eg5 (1–450 aa) were raised in sheep and rabbit using hexahistidine-tagged human proteins expressed in and purified from bacteria. Specific antibodies were purified using the antigens conjugated to Affigel-15. Commercially available antibodies were used to α-tubulin (mouse DM1A; Sigma-Aldrich), Plk1 (mouse SC-17783; Santa Cruz Biotechnology, Inc.), Aurora A (rabbit AB12875; Abcam), Aurora A pT288 (rabbit 3079; Cell Signaling Technology), PPP6C (rabbit A300-844A; Bethyl Laboratories, Inc.), SAPS1–3 (rabbit A300-968A, A300-969A, and A300-972A; Bethyl Laboratories, Inc.), ANKRD28–52 (rabbit A300-974A and A302-372A; Bethyl Laboratories, Inc.), CREST (human auto-antiserum; Europa Bioproducts Ltd.), KID (rabbit AKIN12-A; Cytoskeleton, Inc.), NuMa (mouse AB5673; Abcam), PP1-α (rabbit 2582; Cell Signaling Technology), PP1-β (rabbit A300-905A; Bethyl Laboratories, Inc.), PP1-γ (goat SC-6108; Santa Cruz Biotechnology, Inc.), PP2A (mouse 610555; BD), TPX2 (mouse ab32795; Abcam), Hec1 (mouse GTX70268; GeneTex, Inc.), CenpE (mouse ab5093; Abcam), CenpA (mouse ab13939; Abcam), pericentrin (rabbit ab4448; Abcam), and cyclin B1 (mouse GNS3; Millipore). Aurora A kinase inhibitor was obtained from Selleck Chemicals (MLN8237; 10 mM of 1,000,000× stock). Secondary antibodies raised in donkey to mouse, rabbit, sheep/goat, and human conjugated to HRP, Alexa Fluor 488, Alexa Fluor 555, Alexa Fluor 568, and Alexa Fluor 647 were obtained from Invitrogen and Jackson ImmunoResearch Laboratories, Inc.

Molecular biology

Full-length clones were amplified with the KOD polymerase (Merck) from total HeLa RNA extracted using TRIZOL (Invitrogen). Point mutations were introduced using the QuickChange system (Agilent Technologies) according to the manufacturer's protocol. All primers were obtained from Metabion GmbH. Expression constructs were produced in pcDNA3 vectors modified to encode the chicken β-actin promoter to reduce expression levels, the required tags (EGFP, FLAG, or mCherry), and the geneticin, puromycin, or blasticidin resistance selection markers. The siRNA library targeting human phosphatase subunits and single duplexes corresponding to the individual pools were obtained from Thermo Fisher Scientific and are listed in Table S1.

Cell culture

HeLa and MRC-5 cells were cultured in growth medium (DME containing 10% fetal bovine serum) at 37°C and 5% CO_2. For plasmid transfection and siRNA transfection, LT1 (Mirus Bio, LLC) and Oligofectamine (Invitrogen), respectively, were used according to the manufacturer's instructions. For making stable cell lines, constructs were transfected into HeLa S3 cells. After a 24-h selection, drugs were added as follows: 700 µg/ml geneticin, 1.0 µg/ml puromycin, and 2.0 µg/ml blasticidin. Colonies were picked after a 14-d selection, and expression was checked by Western blotting.

Fixed and live-cell microscopy

Fixed samples on glass slides were imaged using a 60× 1.35 NA oil immersion objective on a standard upright microscope system with filter sets for DAPI, EGFP/Alexa Fluor 488, Alexa Fluor 555, Alexa Fluor 568, and Alexa Fluor 647 (Chroma Technology Corp.), a camera (CoolSNAP HQ2; Roper Industries), and imaging software (MetaMorph 7.5; Molecular Dynamics, Inc.). For live-cell imaging, cells were plated in 35-mm dishes with a 14-mm 1.5 thickness coverglass window on the bottom (MatTek Corporation). For imaging, the dishes were placed in a 37°C and 5% CO_2 environment

chamber on the microscope stage. Imaging was performed using a 60× 1.4 NA oil immersion objective on a standard inverted microscope under the control of MetaMorph 7.5 software or a spinning-disk confocal system (Ultraview Vox; PerkinElmer). A maximum intensity projection of the fluorescent channels was performed. Images were then cropped in ImageJ (National Institutes of Health) and placed into Illustrator CS3 (Adobe Systems, Inc.) to produce the figures.

Isolation of PP6 complexes

Wild-type and catalytically inactive PP6 complexes were isolated from 3 × 15–cm dishes of si08^{Res}PPP6C^{WT}, si08^{Res}PPP6C^{PD} stable HeLa cell lines, or untransfected control cells grown to 60% confluence. The cells were arrested in mitosis with 100 ng/ml nocodazole for 16 h. Mitotic cells were harvested by shake off, washed three times with warm PBS, and then resuspended in warm growth medium. The cells were incubated in a 5% CO_2 incubator at 37°C for 20 min and then washed twice with cold PBS. The cells were lysed in 1 ml of cell lysis buffer (50 mM Tris-HCl, pH 7.4, 150 mM NaCl, and 1% Triton X-100 with protease inhibitor cocktail), left on ice for 20 min, and then centrifuged at 20,000 g_{av} for 20 min at 4°C to remove insoluble debris. To isolate PP6 complexes, 20 µl mouse anti-FLAG M2 agarose beads (A2220; Sigma-Aldrich) were added into 900 µl of cell lysate and rotated at 4°C for 3 h. The beads were washed with cell lysis buffer, and the PP6 complex was eluted with 2× 70 µl of 200 µg/ml FLAG peptide in TBS, pH 7.5, to give E1 and E2 fractions.

Phosphatase and kinase assays

Aurora A–TPX2 complexes for use as a substrate in in vitro phosphatase assays were prepared as follows from 3 x 15–cm dishes of HeLa cells grown to 60% confluence. Cell lysates were prepared as for PP6 isolation except that buffers contained phosphatase inhibitor cocktail 1 (Sigma-Aldrich). For Aurora A complex isolation, 2 µg mouse anti-TPX2 antibody and 60 µl protein G–Sepharose beads were added to 700 µl of cell lysate, and the mixture was rotated at 4°C for 2 h. The beads were washed with lysis buffer and then TBS and aliquoted into five tubes. To each tube, either 20 µl TBS, E1-eluted si08^{Res} PPP6C^{WT} or si08^{Res}PPP6C^{PD} complex, E1-eluted HeLa control, or TBS with 0.5 µl of calf intestinal phosphatase was added. The tubes were incubated at room temperature for 2 h and then boiled for 5 min at 95°C after adding 20 µl of 3× SDS loading buffer. Samples were analyzed by Western blotting on normal gels or gels containing 50 µM Phos-tag reagent (Wako Chemicals USA, Inc.) charged with Mn^{2+} to better resolve phosphorylated from nonphosphorylated forms of the same protein. Quantitations were performed using ImageJ from blots of normal gels because reduced transfer efficiency of phosphorylated relative to nonphosphorylated forms of the same protein from Phos-tag gels was observed.

For in vivo phosphatase assays, 5 × 10–cm dishes of HeLa cells were transfected with control or PPP6C si08 duplexes for 48 h and then treated with 100 ng/ml nocodazole for 16 h. Cells were harvested and lysed as for PP6 complex purification, except that the sample was split into two aliquots, one containing phosphatase inhibitor cocktail 1 and the other without. Cell lysis was left to proceed on ice for 20 min, and then insoluble debris was removed by centrifugation at 20,000 g_{av} for 20 min at 4°C. A 30-µl aliquot of supernatant was kept on ice as an input sample, and Aurora A–TPX2 complexes were immune precipitated from the remaining lysate as described in the previous paragraph. The samples were analyzed by Western blotting, and measurements were performed using ImageJ. For phosphatase subunit siRNA library screening assays, this procedure was scaled down to use individual wells of a 6-well plate, and only cell lysates were analyzed.

For in vitro kinase assays, a modification of a published method was used (Preisinger et al., 2005). Control or Aurora A–TPX2 complexes isolated from 1.6 × 10^6 cells were incubated in 50 mM Tris-HCl, pH 7.3, 50 mM KCl, 10 mM $MgCl_2$, 20 mM β-glycerophosphate, 15 mM EGTA, 100 µM ATP, 0.5 µl γ-[^{32}P]ATP, and 1 µg histone H3 substrate in 20 µl of final volume for 30 min at 30°C. Reactions were analyzed by SDS-PAGE and autoradiography.

Mass spectrometry

Protein samples for mass spectrometry were separated on 4–12% gradient NuPAGE gels and then stained using a colloidal Coomassie blue stain. Gel lanes were cut into 12 slices and then digested with trypsin (Wilm et al., 1996). The resulting tryptic peptide mixtures in 0.05% trifluoroacetic acid were then analyzed by online liquid chromatography with tandem mass spectrometry with a nanoAcquity UPLC system (Waters Corporation) and a mass spectrometer (Orbitrap XL ETD; Thermo Fisher Scientific) fitted with a nanoelectrospray source (Proxeon). Peptides were loaded onto a 5-cm × 180-µm trap column (BEH-C18 Symmetry; Waters Corporation) in 0.1% formic acid at 15 µl/min and then resolved using a 25-cm × 75-µm column using a 20-min linear gradient of 0 to 37.5% acetonitrile in 0.1% formic acid at a flow rate of 400 nl/min. The mass spectrometer was set to acquire a mass spectrometry survey scan in the Orbitrap (resolution = 30,000) and then perform tandem mass spectrometry on the top five multiply charged ions in the linear quadrupole ion trap after fragmentation using collision ionization (30 ms at 35% energy). A 90-s rolling exclusion list with $n = 3$ was used to limit redundant analysis. Maxquant and Mascot (Matrix Science) were then used to compile and search the raw data against the human international protein index database. Protein group and peptide lists were sorted and analyzed in Excel (Microsoft) and Maxquant (Cox and Mann, 2008). Mass spectrometry and tandem mass spectrometry spectra were manually inspected using Xcalibur Qualbrowser (Thermo Fisher Scientific).

Online supplemental material

Fig. S1 shows that there is redundancy between protein phosphatase catalytic subunits during mitosis. Fig. S2 shows that the subunits of the PP6 holoenzyme localize to the cytosol. Fig. S3 shows that kinetochore proteins localize normally and cold-stable kinetochore fibers are still present in PPP6C-depleted cells. Fig. S4 shows increased Aurora A pT288 at the spindle in PPP6C-depleted cells. Fig. S5 shows reduced levels of KIF11/Eg5 at the spindle in the absence of PPP6C. Videos 1 and 2 show the effect of PPP6C depletion on spindle formation and chromosome alignment in living cells. Table S1 contains a list of the siRNA duplexes directed toward phosphatase catalytic and regulatory subunits used in the course of this study. Online supplemental material is available at http://www.jcb.org/cgi/content/full/jcb.201008106/DC1.

We thank Anja Dunsch for commenting on the manuscript, Dean Hammond for help with MaxQuant, and Colin Hornby for initial assistance with live-cell confocal imaging.

This work was supported by a Cancer Research UK career development fellowship to U. Gruneberg (C24085/A8296) and a Cancer Research UK program grant to F.A. Barr (C20079/A9473).

Submitted: 18 August 2010
Accepted: 23 November 2010

References

Adams, J.A. 2003. Activation loop phosphorylation and catalysis in protein kinases: is there functional evidence for the autoinhibitor model? *Biochemistry.* 42:601–607. doi:10.1021/bi020617o

Afshar, K., M.E. Werner, Y.C. Tse, M. Glotzer, and P. Gönczy. 2010. Regulation of cortical contractility and spindle positioning by the protein phosphatase 6 PPH-6 in one-cell stage *C. elegans* embryos. *Development.* 137:237–247. doi:10.1242/dev.042754

Ahonen, L.J., M.J. Kallio, J.R. Daum, M. Bolton, I.A. Manke, M.B. Yaffe, P.T. Stukenberg, and G.J. Gorbsky. 2005. Polo-like kinase 1 creates the tension-sensing 3F3/2 phosphoepitope and modulates the association of spindle-checkpoint proteins at kinetochores. *Curr. Biol.* 15:1078–1089. doi:10.1016/j.cub.2005.05.026

Andrésson, T., and J.V. Ruderman. 1998. The kinase Eg2 is a component of the *Xenopus* oocyte progesterone-activated signaling pathway. *EMBO J.* 17:5627–5637. doi:10.1093/emboj/17.19.5627

Bamford, S., E. Dawson, S. Forbes, J. Clements, R. Pettett, A. Dogan, A. Flanagan, J. Teague, P.A. Futreal, M.R. Stratton, and R. Wooster. 2004. The COSMIC (Catalogue of Somatic Mutations in Cancer) database and website. *Br. J. Cancer.* 91:355–358.

Bayliss, R., T. Sardon, I. Vernos, and E. Conti. 2003. Structural basis of Aurora-A activation by TPX2 at the mitotic spindle. *Mol. Cell.* 12:851–862. doi:10.1016/S1097-2765(03)00392-7

Bischoff, J.R., L. Anderson, Y. Zhu, K. Mossie, L. Ng, B. Souza, B. Schryver, P. Flanagan, F. Clairvoyant, C. Ginther, et al. 1998. A homologue of *Drosophila* aurora kinase is oncogenic and amplified in human colorectal cancers. *EMBO J.* 17:3052–3065. doi:10.1093/emboj/17.11.3052

Bollen, M., D.W. Gerlich, and B. Lesage. 2009. Mitotic phosphatases: from entry guards to exit guides. *Trends Cell Biol.* 19:531–541. doi:10.1016/j.tcb.2009.06.005

Chen, F., V. Archambault, A. Kar, P. Lio', P.P. D'Avino, R. Sinka, K. Lilley, E.D. Laue, P. Deak, L. Capalbo, and D.M. Glover. 2007. Multiple protein phosphatases are required for mitosis in *Drosophila*. *Curr. Biol.* 17:293–303. doi:10.1016/j.cub.2007.01.068

Clarke, P.R., and C. Zhang. 2008. Spatial and temporal coordination of mitosis by Ran GTPase. *Nat. Rev. Mol. Cell Biol.* 9:464–477. doi:10.1038/nrm2410

Cox, J., and M. Mann. 2008. MaxQuant enables high peptide identification rates, individualized p.p.b.-range mass accuracies and proteome-wide protein quantification. *Nat. Biotechnol.* 26:1367–1372. doi:10.1038/nbt.1511

Daum, J.R., and G.J. Gorbsky. 2006. Lysed cell models and isolated chromosomes for the study of kinetochore/centromere biochemistry in vitro. *Methods.* 38:52–59.

DeLuca, J.G., B. Moree, J.M. Hickey, J.V. Kilmartin, and E.D. Salmon. 2002. hNuf2 inhibition blocks stable kinetochore–microtubule attachment and induces mitotic cell death in HeLa cells. *J. Cell Biol.* 159:549–555. doi:10.1083/jcb.200208159

Dohadwala, M., E.F. da Cruz e Silva, F.L. Hall, R.T. Williams, D.A. Carbonaro-Hall, A.C. Nairn, P. Greengard, and N. Berndt. 1994. Phosphorylation and inactivation of protein phosphatase 1 by cyclin-dependent kinases. *Proc. Natl. Acad. Sci. USA.* 91:6408–6412. doi:10.1073/pnas.91.14.6408

Douglas, P., J. Zhong, R. Ye, G.B. Moorhead, X. Xu, and S.P. Lees-Miller. 2010. Protein phosphatase 6 interacts with the DNA-dependent protein kinase catalytic subunit and dephosphorylates gamma-H2AX. *Mol. Cell. Biol.* 30:1368–1381. doi:10.1128/MCB.00741-09

Eckerdt, F., P.A. Eyers, A.L. Lewellyn, C. Prigent, and J.L. Maller. 2008. Spindle pole regulation by a discrete Eg5-interacting domain in TPX2. *Curr. Biol.* 18:519–525. doi:10.1016/j.cub.2008.02.077

Eyers, P.A., and J.L. Maller. 2004. Regulation of *Xenopus* Aurora A activation by TPX2. *J. Biol. Chem.* 279:9008–9015. doi:10.1074/jbc.M312424200

Eyers, P.A., E. Erikson, L.G. Chen, and J.L. Maller. 2003. A novel mechanism for activation of the protein kinase Aurora A. *Curr. Biol.* 13:691–697. doi:10.1016/S0960-9822(03)00166-0

Forbes, S.A., G. Tang, N. Bindal, S. Bamford, E. Dawson, C. Cole, C.Y. Kok, M. Jia, R. Ewing, A. Menzies, et al. 2010. COSMIC (the Catalogue of Somatic Mutations in Cancer): a resource to investigate acquired mutations in human cancer. *Nucleic Acids Res.* 38(suppl. 1):D652–D657. doi:10.1093/nar/gkp995

Giet, R., R. Uzbekov, F. Cubizolles, K. Le Guellec, and C. Prigent. 1999. The *Xenopus laevis* aurora-related protein kinase pEg2 associates with and phosphorylates the kinesin-related protein XlEg5. *J. Biol. Chem.* 274:15005–15013. doi:10.1074/jbc.274.21.15005

Giet, R., D. McLean, S. Descamps, M.J. Lee, J.W. Raff, C. Prigent, and D.M. Glover. 2002. *Drosophila* Aurora A kinase is required to localize D-TACC to centrosomes and to regulate astral microtubules. *J. Cell Biol.* 156:437–451. doi:10.1083/jcb.200108135

Glover, D.M., M.H. Leibowitz, D.A. McLean, and H. Parry. 1995. Mutations in aurora prevent centrosome separation leading to the formation of monopolar spindles. *Cell.* 81:95–105. doi:10.1016/0092-8674(95)90374-7

Gold, M.G., D. Barford, and D. Komander. 2006. Lining the pockets of kinases and phosphatases. *Curr. Opin. Struct. Biol.* 16:693–701. doi:10.1016/j.sbi.2006.10.006

Goshima, G., O. Iwasaki, C. Obuse, and M. Yanagida. 2003. The role of Ppe1/PP6 phosphatase for equal chromosome segregation in fission yeast kinetochore. *EMBO J.* 22:2752–2763. doi:10.1093/emboj/cdg266

Hartshorne, D.J., M. Ito, and F. Erdödi. 2004. Role of protein phosphatase type 1 in contractile functions: myosin phosphatase. *J. Biol. Chem.* 279:37211–37214. doi:10.1074/jbc.R400018200

Hirano, K., B.C. Phan, and D.J. Hartshorne. 1997. Interactions of the subunits of smooth muscle myosin phosphatase. *J. Biol. Chem.* 272:3683–3688. doi:10.1074/jbc.272.6.3683

Hirota, T., N. Kunitoku, T. Sasayama, T. Marumoto, D. Zhang, M. Nitta, K. Hatakeyama, and H. Saya. 2003. Aurora-A and an interacting activator, the LIM protein Ajuba, are required for mitotic commitment in human cells. *Cell.* 114:585–598. doi:10.1016/S0092-8674(03)00642-1

Huse, M., and J. Kuriyan. 2002. The conformational plasticity of protein kinases. *Cell.* 109:275–282. doi:10.1016/S0092-8674(02)00741-9

Hutterer, A., D. Berdnik, F. Wirtz-Peitz, M. Zigman, A. Schleiffer, and J.A. Knoblich. 2006. Mitotic activation of the kinase Aurora-A requires its binding partner Bora. *Dev. Cell.* 11:147–157. doi:10.1016/j.devcel.2006.06.002

Jang, Y.J., S. Ma, Y. Terada, and R.L. Erikson. 2002. Phosphorylation of threonine 210 and the role of serine 137 in the regulation of mammalian polo-like kinase. *J. Biol. Chem.* 277:44115–44120. doi:10.1074/jbc.M202172200

Johnson, D.F., G. Moorhead, F.B. Caudwell, P. Cohen, Y.H. Chen, M.X. Chen, and P.T. Cohen. 1996. Identification of protein-phosphatase-1-binding domains on the glycogen and myofibrillar targetting subunits. *Eur. J. Biochem.* 239:317–325. doi:10.1111/j.1432-1033.1996.0317u.x

Johnson, G.L., D.L. Brautigan, C. Shriner, S. Jaspers, J. Arino, J.E. Mole, T.B. Miller Jr., and M.C. Mumby. 1987. Sequence homologies between type 1 and type 2A protein phosphatases. *Mol. Endocrinol.* 1:745–748. doi:10.1210/mend-1-10-745

Karthigeyan, D., S.B. Prasad, J. Shandilya, S. Agrawal, and T.K. Kundu. 2010. Biology of Aurora A kinase: Implications in cancer manifestation and therapy. *Med. Res. Rev.*

Kinoshita, K., T.L. Noetzel, L. Pelletier, K. Mechtler, D.N. Drechsel, A. Schwager, M. Lee, J.W. Raff, and A.A. Hyman. 2005. Aurora A phosphorylation of TACC3/maskin is required for centrosome-dependent microtubule assembly in mitosis. *J. Cell Biol.* 170:1047–1055. doi:10.1083/jcb.200503023

Kitajima, T.S., T. Sakuno, K. Ishiguro, S. Iemura, T. Natsume, S.A. Kawashima, and Y. Watanabe. 2006. Shugoshin collaborates with protein phosphatase 2A to protect cohesin. *Nature.* 441:46–52. doi:10.1038/nature04663

Kong, M., D. Ditsworth, T. Lindsten, and C.B. Thompson. 2009. Alpha4 is an essential regulator of PP2A phosphatase activity. *Mol. Cell.* 36:51–60. doi:10.1016/j.molcel.2009.09.025

Kufer, T.A., H.H. Silljé, R. Körner, O.J. Gruss, P. Meraldi, and E.A. Nigg. 2002. Human TPX2 is required for targeting Aurora-A kinase to the spindle. *J. Cell Biol.* 158:617–623. doi:10.1083/jcb.200204155

Kwon, Y.G., S.Y. Lee, Y. Choi, P. Greengard, and A.C. Nairn. 1997. Cell cycle-dependent phosphorylation of mammalian protein phosphatase 1 by cdc2 kinase. *Proc. Natl. Acad. Sci. USA.* 94:2168–2173. doi:10.1073/pnas.94.6.2168

Lane, H.A., and E.A. Nigg. 1996. Antibody microinjection reveals an essential role for human polo-like kinase 1 (Plk1) in the functional maturation of mitotic centrosomes. *J. Cell Biol.* 135:1701–1713. doi:10.1083/jcb.135.6.1701

Llamazares, S., A. Moreira, A. Tavares, C. Girdham, B.A. Spruce, C. Gonzalez, R.E. Karess, D.M. Glover, and C.E. Sunkel. 1991. polo encodes a protein kinase homolog required for mitosis in *Drosophila*. *Genes Dev.* 5:2153–2165. doi:10.1101/gad.5.12a.2153

Luo, J., M.J. Emanuele, D. Li, C.J. Creighton, M.R. Schlabach, T.F. Westbrook, K.K. Wong, and S.J. Elledge. 2009. A genome-wide RNAi screen identifies multiple synthetic lethal interactions with the Ras oncogene. *Cell.* 137:835–848. doi:10.1016/j.cell.2009.05.006

Manfredi, M.G., J.A. Ecsedy, K.A. Meetze, S.K. Balani, O. Burenkova, W. Chen, K.M. Galvin, K.M. Hoar, J.J. Huck, P.J. LeRoy, et al. 2007. Antitumor activity of MLN8054, an orally active small-molecule inhibitor of Aurora A kinase. *Proc. Natl. Acad. Sci. USA.* 104:4106–4111. doi:10.1073/pnas.0608798104

Mi, J., J. Dziegielewski, E. Bolesta, D.L. Brautigan, and J.M. Larner. 2009. Activation of DNA-PK by ionizing radiation is mediated by protein phosphatase 6. *PLoS One.* 4:e4395. doi:10.1371/journal.pone.0004395

Nigg, E.A. 2001. Mitotic kinases as regulators of cell division and its checkpoints. *Nat. Rev. Mol. Cell Biol.* 2:21–32. doi:10.1038/35048096

Ohashi, S., G. Sakashita, R. Ban, M. Nagasawa, H. Matsuzaki, Y. Murata, H. Taniguchi, H. Shima, K. Furukawa, and T. Urano. 2006. Phosphoregulation of human protein kinase Aurora-A: analysis using anti-phospho-Thr288 monoclonal antibodies. *Oncogene.* 25:7691–7702. doi:10.1038/sj.onc.1209754

Ozlü, N., M. Srayko, K. Kinoshita, B. Habermann, E.T. O'Toole, T. Müller-Reichert, N. Schmalz, A. Desai, and A.A. Hyman. 2005. An essential function of the *C. elegans* ortholog of TPX2 is to localize activated aurora A kinase to mitotic spindles. *Dev. Cell.* 9:237–248. doi:10.1016/j.devcel.2005.07.002

Preisinger, C., R. Körner, M. Wind, W.D. Lehmann, R. Kopajtich, and F.A. Barr. 2005. Plk1 docking to GRASP65 phosphorylated by Cdk1 suggests a mechanism for Golgi checkpoint signalling. *EMBO J.* 24:753–765. doi:10.1038/sj.emboj.7600569

Prickett, T.D., and D.L. Brautigan. 2006. The alpha4 regulatory subunit exerts opposing allosteric effects on protein phosphatases PP6 and PP2A. *J. Biol. Chem.* 281:30503–30511. doi:10.1074/jbc.M601054200

Roghi, C., R. Giet, R. Uzbekov, N. Morin, I. Chartrain, R. Le Guellec, A. Couturier, M. Dorée, M. Philippe, and C. Prigent. 1998. The *Xenopus* protein kinase pEg2 associates with the centrosome in a cell cycle-dependent manner, binds to the spindle microtubules and is involved in bipolar mitotic spindle assembly. *J. Cell Sci.* 111:557–572.

Satinover, D.L., C.A. Leach, P.T. Stukenberg, and D.L. Brautigan. 2004. Activation of Aurora-A kinase by protein phosphatase inhibitor-2, a bifunctional signaling protein. *Proc. Natl. Acad. Sci. USA.* 101:8625–8630. doi:10.1073/pnas.0402966101

Sen, S., H. Zhou, and R.A. White. 1997. A putative serine/threonine kinase encoding gene BTAK on chromosome 20q13 is amplified and overexpressed in human breast cancer cell lines. *Oncogene.* 14:2195–2200. doi:10.1038/sj.onc.1201065

Sessa, F., M. Mapelli, C. Ciferri, C. Tarricone, L.B. Areces, T.R. Schneider, P.T. Stukenberg, and A. Musacchio. 2005. Mechanism of Aurora B activation by INCENP and inhibition by hesperadin. *Mol. Cell.* 18:379–391. doi:10.1016/j.molcel.2005.03.031

Shi, Y. 2009. Serine/threonine phosphatases: mechanism through structure. *Cell.* 139:468–484. doi:10.1016/j.cell.2009.10.006

Stefansson, B., and D.L. Brautigan. 2006. Protein phosphatase 6 subunit with conserved Sit4-associated protein domain targets IkappaBepsilon. *J. Biol. Chem.* 281:22624–22634. doi:10.1074/jbc.M601772200

Stefansson, B., T. Ohama, A.E. Daugherty, and D.L. Brautigan. 2008. Protein phosphatase 6 regulatory subunits composed of ankyrin repeat domains. *Biochemistry.* 47:1442–1451. doi:10.1021/bi7022877

Tang, Z., H. Shu, W. Qi, N.A. Mahmood, M.C. Mumby, and H. Yu. 2006. PP2A is required for centromeric localization of Sgo1 and proper chromosome segregation. *Dev. Cell.* 10:575–585. doi:10.1016/j.devcel.2006.03.010

Terrak, M., F. Kerff, K. Langsetmo, T. Tao, and R. Dominguez. 2004. Structural basis of protein phosphatase 1 regulation. *Nature.* 429:780–784. doi:10.1038/nature02582

Tóth, A., E. Kiss, F.W. Herberg, P. Gergely, D.J. Hartshorne, and F. Erdödi. 2000. Study of the subunit interactions in myosin phosphatase by surface plasmon resonance. *Eur. J. Biochem.* 267:1687–1697. doi:10.1046/j.1432-1327.2000.01158.x

Tsai, M.Y., C. Wiese, K. Cao, O. Martin, P. Donovan, J. Ruderman, C. Prigent, and Y. Zheng. 2003. A Ran signalling pathway mediated by the mitotic kinase Aurora A in spindle assembly. *Nat. Cell Biol.* 5:242–248. doi:10.1038/ncb936

Vagnarelli, P., D.F. Hudson, S.A. Ribeiro, L. Trinkle-Mulcahy, J.M. Spence, F. Lai, C.J. Farr, A.I. Lamond, and W.C. Earnshaw. 2006. Condensin and Repo-Man-PP1 co-operate in the regulation of chromosome architecture during mitosis. *Nat. Cell Biol.* 8:1133–1142. doi:10.1038/ncb1475

Walter, A.O., W. Seghezzi, W. Korver, J. Sheung, and E. Lees. 2000. The mitotic serine/threonine kinase Aurora2/AIK is regulated by phosphorylation and degradation. *Oncogene.* 19:4906–4916. doi:10.1038/sj.onc.1203847

Wilm, M., A. Shevchenko, T. Houthaeve, S. Breit, L. Schweigerer, T. Fotsis, and M. Mann. 1996. Femtomole sequencing of proteins from polyacrylamide gels by nano-electrospray mass spectrometry. *Nature.* 379:466–469. doi:10.1038/379466a0

Xing, Y., Y. Xu, Y. Chen, P.D. Jeffrey, Y. Chao, Z. Lin, Z. Li, S. Strack, J.B. Stock, and Y. Shi. 2006. Structure of protein phosphatase 2A core enzyme bound to tumor-inducing toxins. *Cell.* 127:341–353. doi:10.1016/j.cell.2006.09.025

Yamashiro, S., Y. Yamakita, G. Totsukawa, H. Goto, K. Kaibuchi, M. Ito, D.J. Hartshorne, and F. Matsumura. 2008. Myosin phosphatase-targeting subunit 1 regulates mitosis by antagonizing polo-like kinase 1. *Dev. Cell.* 14:787–797. doi:10.1016/j.devcel.2008.02.013

Zhao, Z.S., J.P. Lim, Y.W. Ng, L. Lim, and E. Manser. 2005. The GIT-associated kinase PAK targets to the centrosome and regulates Aurora-A. *Mol. Cell.* 20:237–249. doi:10.1016/j.molcel.2005.08.035

Zhou, H., J. Kuang, L. Zhong, W.L. Kuo, J.W. Gray, A. Sahin, B.R. Brinkley, and S. Sen. 1998. Tumour amplified kinase STK15/BTAK induces centrosome amplification, aneuploidy and transformation. *Nat. Genet.* 20:189–193. doi:10.1038/2496